



Terra/Aqua – MODIS (Moderate Resolution Imaging Spectroradiometer) image of the eastern Great Lakes region on February 28, 2004. White sheets of ice float on Lake Huron, top left, and Lake Erie, bottom center. Lake Ontario, right, remains free of ice because of its depth, though the land around it is in winter's icy grip. The mean depth is 19 m in Lake Erie and 86 m in Lake Ontario.

NASA. Production by The Visible Earth team (<http://visibleearth.nasa.gov/>).

## 2.1 Lake Types and Characteristics

### 2.1.1 Classification and Geometry of Lakes

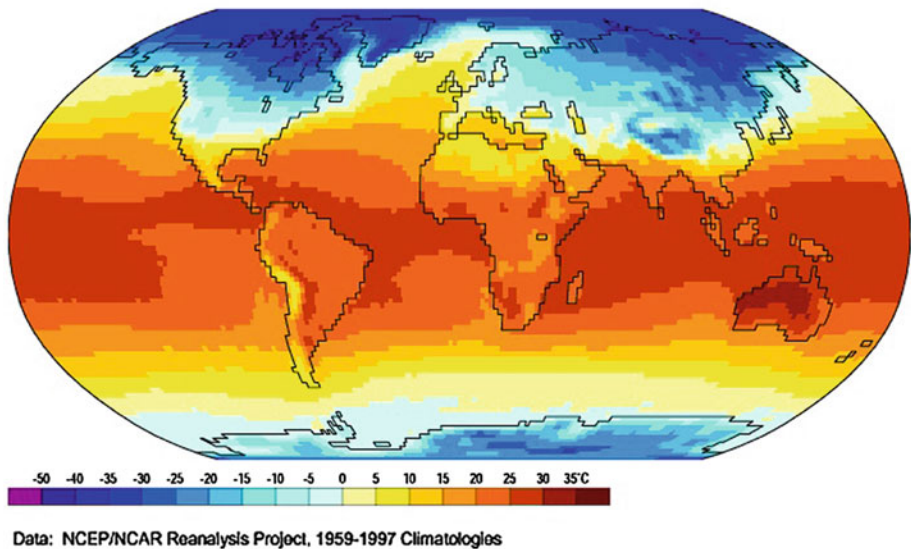
Lakes are found in all climate zones. A first-order zonation of potentially freezing freshwater lakes can be taken as the continental areas where the January (Northern Hemisphere) or July (Southern Hemisphere) mean air temperature is less than 0 °C (Fig. 2.1). This region is called the *cold climate zone* in the present book. There, at least very shallow freshwater lakes freeze in normal years (Fig. 2.2). The cold climate zone covers most of Eurasia and North America down to around 40°N at sea level (see Hutchinson and Löffler 1956; Bates and Bilello 1966). In the Asian mountains the boundary is more south, while in the Western Europe it is more north. Apart from Antarctica, in the Southern Hemisphere only some mountain areas are included in the zone of freezing lakes. Actually, between 45°S and the Antarctic continent the only land masses are the southern corner of New Zealand and some small islands with eventual minor freezing inland water basins; e.g., Lake Alta, a small and deep cirque lake in the New Zealand Southern Alps at 45°03'S 168°49'E, 1,800 m above sea level. In the high Andes, the cold zone even reaches the Equator.

However, in the cold climate zone there are lakes, which do not freeze. Very deep lakes have thermal time scale longer than the winter, geothermal heating influences the surface temperature due to convective mixing in the water body, and salinity depresses the freezing point. Examples of these lakes are the very deep Lake Shikotsu (mean depth 266 m) in Hokkaido (<http://www.ilec.or.jp/database/asi/asi-16.html>), the geothermal Lake Hévíz in Hungary, where the water temperature is above 20 °C in winter although other lakes in the region are normally frozen (<http://www.lakeheviz.hu>), and the hypersaline Don Juan Pond (salinity 440 ‰) in McMurdo Dry Valley in Antarctica, generally unfrozen in winter even at temperatures below –50 °C (Meyer et al. 1962).

For lake ice climatology, it is convenient to define *the ice year* as the time between the maxima in the summer heat storage in two consequent summers. In the Northern Hemisphere the maximum occurs normally in July–August, while in the south it is January–February. The ice years are labelled as the year they begin, i.e. ice year 2006 is the period between the summer maxima of 2006 and 2007. In this way ice-free years and *perennial ice* periods can be properly treated in ice phenology analyses. Perennial ice or *multi-year ice* is ice that has survived at least one summer, while ice-free ice year is such where no ice occurs between two summer maxima.

A natural *geological classification* of lakes is according to the origins of the depressions, where lakes have formed (Table 2.1). The time scale of the depressions is usually very long. On a short time-scale, new ones can be created by landslides or environmental engineering. The formation of glacial lakes has taken place at glaciers and ice sheets. In the Northern Europe and North America there are large lake districts, which originate from ice sheet–land processes after the Last Glacial Maximum. Epiglacial, supraglacial and subglacial lakes constitute the class of proglacial lakes, which are found at existing

(a)



(b)

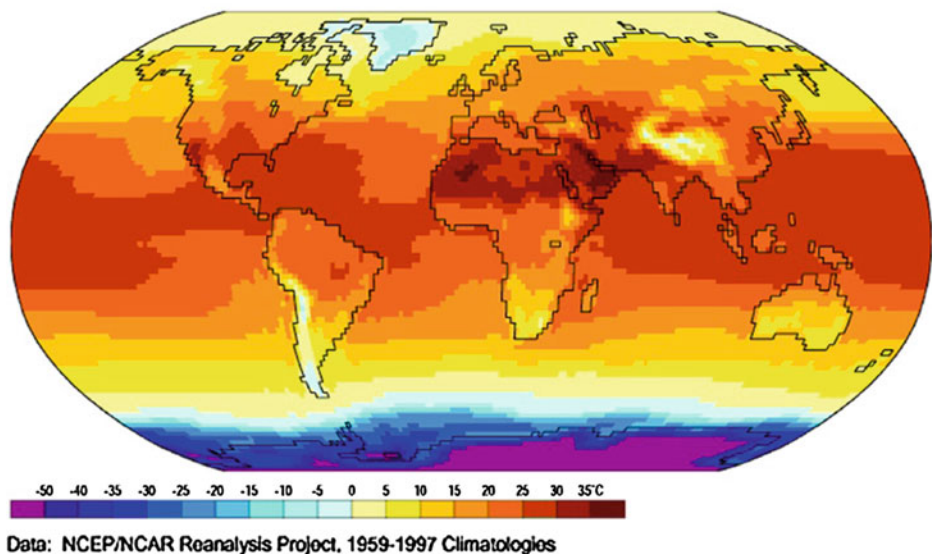


**Fig. 2.1** Mean **a** January and **b** July air temperature (°C) on the Earth's surface, 1959–1997 (Global climate animations, Department of Geography, University of Oregon based on NCEP/NCAR Reanalysis Project 1959–1997 Climatologies data, see [http://geography.uoregon.edu/envchange/clim\\_animations/index.html](http://geography.uoregon.edu/envchange/clim_animations/index.html)). © Department of Geography, University of Oregon

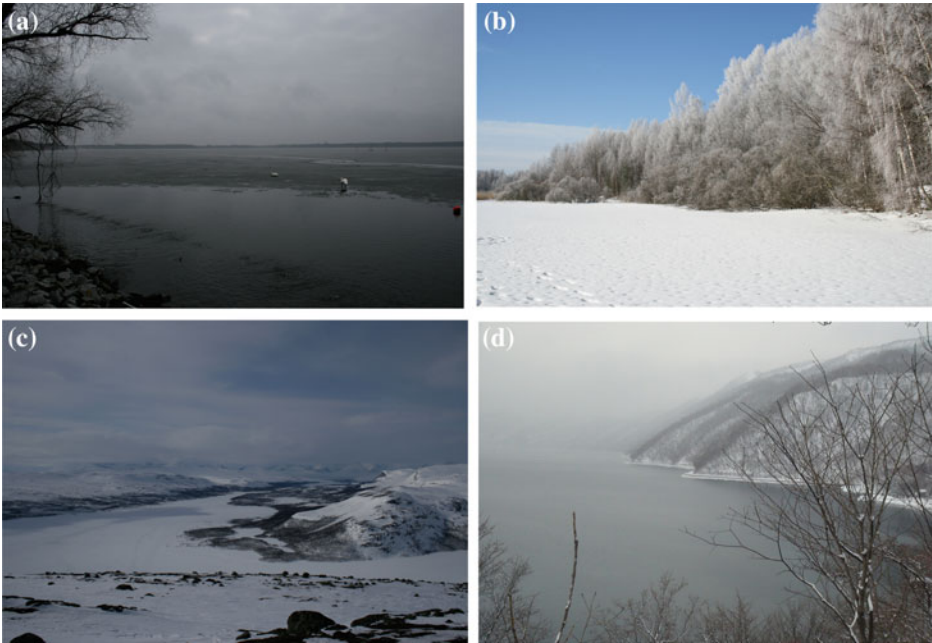


**Fig. 2.2** Lakes in the cold climate zone: **a** Ephemeral, Lake Müggelsee, Berlin; **b** Boreal, Lake Pääjärvi, southern Finland; **c** Tundra, Lake Kilpisjärvi, Lapland; **d** Deep, non-freezing lake, Lake Shikotsu, Hokkaido

**Table 2.1** The origins of lake basins with examples from the cold climate zone

Class	Mechanism for depression	Examples
Tectonic	Plate shifts	Lake Baikal (Russia)
Volcanic	Volcano crater	Lake Shikotsu (Hokkaido, Japan)
Meteorite	Impact crater	Lake Lappajärvi (Finland)
Landslide	Land mass accumulation	Attabad Lake (Pakistan)
Reservoir	Man-made	Rybinsk reservoir (Volga basin, Russia)
Glacial	Ice sheet dynamics	Lake Saimaa (Finland)
Epiglacial	Ice sheet dynamics	Lake Mandrone (Italy)
Supraglacial	Solar radiation	Lake Suvivesi (Dronning Maud Land)
Subglacial	Glacial pressure	Lake Vostok (East Antarctica)

glaciers and ice sheets, and glacial meltwater forms the main part of their water balance. Supraglacial lakes are a particular category in that their base is ice rather than rock or soil. Sometimes epishelf lakes are taken as their own category, accounting for freshwater lakes at the surface of ice shelves and a marine basin underneath.

**Example 2.1.** The Baltic Sea has a dynamic history since the retreat of the Fennoscandian ice sheet, beginning 15,000 years ago, due to the positive fresh water balance and rebound of the ground from the pressure of the ice sheet (see Leppäranta and Myrberg 2009). First, the basin was an epiglacial lake (the Baltic Ice Lake), then a brackish sea (the Yoldia Sea, connected to Atlantic), and again an epiglacial lake (Ancylus Lake, Fig. 2.3). About 8,000 years ago Ancylus Lake turned into a brackish marine basin, which has developed to the present Baltic Sea. The land uplift is still in progress in the northern Baltic Sea, and after 1,000 years the northern basin, the Bay of Bothnia, will be isolated from the oceanic connection and become the largest lake in Europe. The presently largest lake of Europe, Lake Ladoga, was part of the Baltic Ice Lake but became isolated in the Yoldia Sea phase.

The *physical classification* of the lake basins concerns their size and shape. A simple approach is to consider the magnitudes of the geometric size, both horizontal and vertical

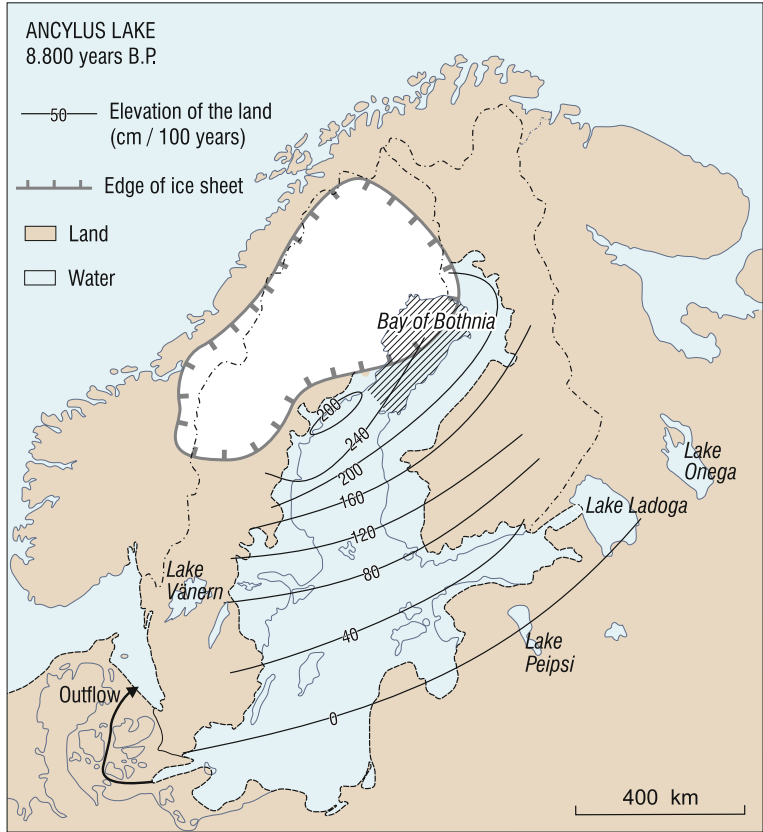


**Fig. 2.3** Ancylus Lake. Also shown are the largest lake of Europe, the Lake Ladoga, which separated at the formation of the Yoldia Sea about 10,000 years ago, and the Bay of Bothnia, the largest lake in Europe after 1,000 years. The contour inside the lake shows the present Baltic Sea. Modified from Leppäranta and Myrberg (2009)

extent. The following system corresponds to the present terminology as well as to the common language (Table 2.2).

**Table 2.2** Classification of lakes for their lateral and vertical size

Lateral	Very large	Large	Medium	Small	Very small
	1,000 km	100 km	10 km	1 km	100 m
Vertical	Very deep	Deep		Shallow	Very shallow
	1,000 m	100 m		10 m	1 m

*Note* ‘medium deep’ concept is not used for lakes in general

The lateral dimension is taken as the length of the major axis of the lake,  $\ell_{\max}$ , and the vertical dimension is taken as the maximum depth  $H_{\max}$ . Lakes with horizontal extent much smaller than 100 m are ponds or pools. The minor axis  $\ell_{\min}$  is defined as the minimum width of the ‘opening’ through which the lake could penetrate. These two axes together with the area and depth define the elongation  $\gamma$ , the shape factor  $\kappa$ , and the aspect ratio  $\delta$ :

$$\gamma = \frac{\ell_{\max}}{\ell_{\min}}, \quad \kappa = \frac{A}{\ell_{\max} \ell_{\min}}, \quad \delta = \frac{H_{\max}}{\ell_{\max}} \quad (2.1)$$

where  $A$  is the surface area of the lake. For a square lake,  $\gamma = 1$ , and for a rectangular lake  $\kappa = 1$ . The aspect ratio is normally  $\delta \sim 10^{-3}$ . Example medium-size lakes have depth of 10 m and lateral extent of 10 km. Lakes are defined open or closed whether there is outflow or not, respectively.

The horizontal size of a lake influences the mixing conditions, since long wind fetches create more turbulence and higher waves. Freshwater lakes are vertically mixed at the temperature of maximum density, and therefore the depth of a lake is one of the principal characteristics to influence the timing of the freezing. The deeper or larger the lake, the later will the freezing be and, consequently, the shorter the ice season. In brackish and saline lakes, the temperature of maximum density depends on the salinity and mixing by cooling reaches halocline. In the freeze-up of a lake, the distribution of depth influences the lateral growth of the ice cover. The whole depth distribution is given by the hypso-graphic curve

$$\Pi(H) = \int_H^{\infty} \pi(H') dH' \quad (2.2)$$

where  $\Pi(H)$  is the relative are of the lake deeper than  $H$ , and  $\pi$  is the spatial density of depth.

A single lake is connected so that liquid water particles can circulate throughout. There may be sub-basins with straits between, and sometimes such basins are taken as separate lakes. The geometry of lakes has fractal characteristics (Korvin 1992). The length of the



**Table 2.3** Classification of lakes based on the salinity ( $S$ ) of the water

Freshwater lakes	$S < 0.5 \text{ ‰}$	Salinity of concern only in ice season
Brackish lakes	$0.5 \text{ ‰} \leq S < 24.6 \text{ ‰}$	Freezing point < temperature of max density
Saline lakes	$24.6 \text{ ‰} \leq S < 35 \text{ ‰}$	Freezing point $\geq$ temperature of max density, salinity at most at the oceanic level
Hypersaline lakes	$S \geq 35 \text{ ‰}$	Salinity greater than the oceanic level

shoreline increases as a power law  $l \propto (\Delta s)^{1-D}$ , where  $D > 1$  is the fractal dimension or the Hausdorff dimension of the shoreline; thus  $l \rightarrow \infty$  as  $\Delta s \rightarrow 0$ . Therefore the length of the shoreline is not a well-defined geometrical property of a lake. Similarly, the number of lakes in an area depends on the resolution of the map and is a questionable quantity. Instead, the surface area and the lengths of the major and minor axes of a lake are well defined. Apart from the descriptive geometry, however, the fractal concept has not brought much new applicable information to lake research. It is clear that the coastline geometry is an important factor during the ice season but the length scale of this factor is finite and process dependent.

The *geochemical classification* of the water quality is firstly based on the salinity<sup>1</sup> ( $S$ ), which is, by definition, the relative mass of dissolved salts and expressed in parts per thousand or per mille (‰). Salinity is a state variable of natural waters and influences on the mixing, circulation, cooling, and freezing. The classification reads (Table 2.3).

Brackish water salinity is much less than the salinity of normal seawater (35 ‰); the transition at 24.6 ‰ is often chosen, because this is the salinity where the temperature of maximum density equals the freezing point (see Sect. 2.1.2). The chemical composition of the lake water plays an especially significant role in hypersaline lakes, for which lake-specific equations of state would be desirable to describe the growth and properties of the ice. Additional geochemical classifiers are pH and concentrations of specific substances; e.g., oxygen, nutrients, organic matter. A specific class of lakes are tidal lakes, such as lagoons, which exchange water with the ocean (Shirasawa et al. 2005). In the northern part of the Baltic Sea, due to glacial land uplift lakes become slowly isolated from the sea and the salinity consequently decreases (e.g., Lindholm et al. 1989). These lakes are called *fladas*.

### 2.1.2 Physical Properties of Lake Waters

A fundamental property of lake water is its density, denoted by  $\rho$ . This is provided by the equation of state, which is written in general form as

$$\rho = \rho(T, S, p) \quad (2.3)$$

<sup>1</sup> In limnology, the amount of dissolved salts ( $c_d$ ) is normally expressed in mass/volume (grams/litre). Clearly  $c_d = \rho S$ , where  $\rho$  is the density of the solution.

where  $T$  is temperature and  $p$  is pressure.<sup>2</sup> Salinity is usually ignored in the case of fresh-water bodies, but even there it may be significant under a complete ice cover when turbulence is absent. Results from marine research are mainly used to obtain the properties of water in brackish and saline lakes. Seawater is a chemically uniform solution, where only the total concentration of dissolved salts varies, but lake waters are lake-specific, and therefore each lake would need an own equation of state. However, the seawater case is usually taken as the approximation. Standard seawater formulae are valid for the salinity range from 0 to 40 ‰, and therefore another approach needs to be employed for hypersaline lakes. The influence of pressure on density is significant only in very deep lakes.

The equation of state of seawater is an empirical function with about 40 parameters (UNESCO 1981, see Appendix 1). It can be formulated as:

$$\rho(T, S, p) = \frac{\rho(T, 0, 0) + \Delta(T, S, 0)}{1 - p/K(T, S, p)} \quad (2.4)$$

where  $\rho(T, 0, 0)$  is the density of pure water and  $\Delta(T, S, 0)$  is salinity correction at zero gauge pressure, and the secant bulk modulus  $K = K(T, S, p)$  gives the pressure effect.

The pressure distribution in a lake can be obtained from the hydrostatic law

$$\frac{dp}{dz} = -\rho g \quad (2.5)$$

where  $z$  is the vertical co-ordinate positive up, and  $g = 9.81 \text{ m s}^{-2}$  is the acceleration due to gravity. The surface ( $z = \zeta$ ) boundary condition for the gauge pressure is  $p(\zeta) = 0$ ; note that  $\zeta - z$  is the depth below the lake surface, and if the density is constant, we have  $p = \rho g \cdot (\zeta - z)$ . In fresh water,  $p(10 \text{ m}) = 0.98 \text{ bar}$ , i.e. a 10-m water column corresponds approximately to the pressure of one standard atmosphere  $\approx 1 \text{ bar}$ . Since  $K \approx 2 \times 10^4 \text{ bar}$ , the density increase due to pressure is about 0.5 % per 10 kbar or about 1 km depth. The pressure effect can be ignored in lakes less than 100 m deep ( $p < 10 \text{ bar}$ ).

In deep lakes also the *adiabatic temperature change* is an important factor in the vertical stratification. When a water parcel rises up, its temperature decreases due to decreasing pressure, and in sinking down adiabatic warming takes place in a symmetric manner. The adiabatic change of temperature can be expressed as  $\Gamma \equiv -dT/dz|_{\text{ad}} = \alpha g T / c_p$ , where  $\alpha$  is the coefficient of thermal expansion, and  $c_p$  is the specific heat at constant pressure (see Curry and Webster 1999); in fresh water,  $\Gamma \sim 0.12 \text{ }^\circ\text{C km}^{-1}$ . The temperature corresponding to the surface temperature after adiabatic cooling is called the *potential temperature*. In a neutrally stratified deep fresh water lake, the potential temperature is constant, and therefore the in situ temperature increases by the adiabatic lapse rate with depth.

---

<sup>2</sup> Pressure is taken as the ‘gauge pressure’, which is the pressure above the sea level atmospheric pressure. Usually pressure is given in bars; the SI unit is Pascal and  $1 \text{ bar} = 100 \text{ kPa}$ . The pressure of one standard atmosphere is 1013.25 mbars.



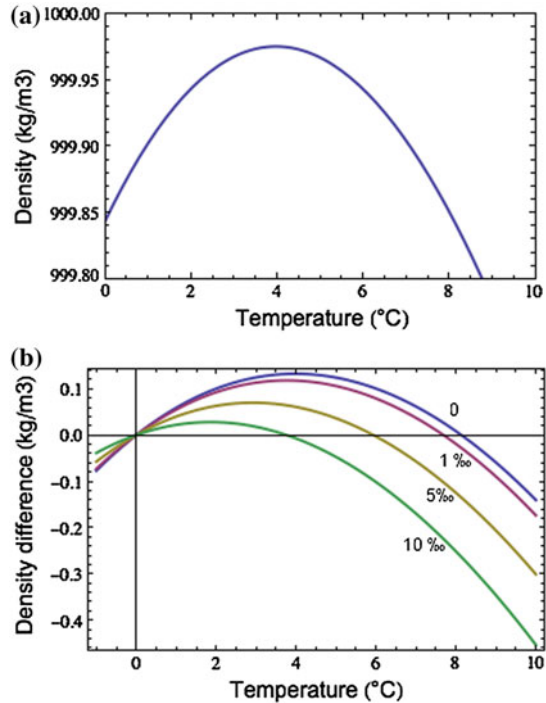
When salinity variations are ignored, the following simple form can be used for the density of lake water:

$$\rho(T, 0, 0) = \rho_0 - \alpha(T - T_m)^2 \quad (2.6)$$

where  $\rho_0 = \rho(T_m, 0, 0) = 999.98 \text{ kg m}^{-3}$  is the fixed reference density,  $T_m$  is the temperature of maximum density of fresh water,  $T_m(S = 0, p = 0) = 3.98 \text{ }^\circ\text{C}$ , and  $\alpha \approx 8.0 \times 10^{-3} \text{ kg m}^{-3} \text{ }^\circ\text{C}^{-2}$  is an empirical parameter (Fig. 2.4). The parameter  $\alpha$  can be further tuned fitting the density to the UNESCO (1981) formula after selecting the applicable temperature range. The first-order approximation for low salinities is obtained just by adding the term  $\beta \cdot S$ ,  $\beta \approx 0.81 \text{ kg m}^{-3}$  to the right-hand side of Eq. (2.6). In cold waters the influence of temperature on density is at smallest. Under a stable ice cover, even small salinity variations can be important, and then it is better to stick to the full UNESCO (1981) formula.

**Example 2.2.** The average density of a human body is  $1,062 \text{ kg m}^{-3}$  (Krywicki and Chinn 1966). If the water salinity is more than 75 ‰, the water is denser and human bodies float free. There are many hypersaline lakes, which satisfy this requirement, perhaps the most famous ones are the Dead Sea ( $S \approx 315 \text{ ‰}$ ,  $\rho \approx 1,240 \text{ kg m}^{-3}$ ) and the Great Salt Lake in Utah ( $S \sim 100 \text{ ‰}$ ,  $\rho \sim 1,100 \text{ kg m}^{-3}$ ).

**Fig. 2.4** Density of water as a function of temperature for different salinities at zero gauge pressure: **a** Pure water density as a function of temperature, **b** Density difference from the density at  $0 \text{ }^\circ\text{C}$  in fresh and brackish water (salinities 0, 1, 5 and 10 ‰). The plots are based on the UNESCO (1981) standard equation of state



Salinity and pressure also influence on the temperature of maximum density and the freezing point,  $T_f$ . The former can be obtained from the equation of state (Eq. 2.4) (in principle, but the mathematics is cumbersome and lower order fits are therefore employed), while the latter is an independent formula given in UNESCO (1981). The fit for  $T_m$  by Caldwell (1978) and the UNESCO freezing point formula are:

$$T_m[^\circ\text{C}] = 3.982 - 0.2229 \cdot S - 0.02004 \cdot p \cdot (1 + 0.00376 \cdot S) \cdot (1 + 0.000402 \cdot p) \quad (2.7a)$$

$$T_f[^\circ\text{C}] = -0.0575 \cdot S + 1.710523 \times 10^{-3} S^{3/2} - 2.154996 \times 10^{-4} S^2 - 7.53 \times 10^{-3} p \quad (2.7b)$$

where the salinity is taken in parts per thousand (‰) and the pressure in bars. These equations are valid for the salinity up to 40 ‰, where  $T_f = -2.21^\circ\text{C}$  and  $T_m = -4.93^\circ\text{C}$  at the zero gauge pressure. It is seen that both the freezing point and the temperature of maximum density decrease with increasing salinity, the latter one even more rapidly. For  $p = 0$ , the curves meet at  $T = -1.28^\circ\text{C}$ ,  $S = 24.6$  ‰. This salinity is normally taken as the boundary between brackish and saline waters; then in brackish water  $T_m \geq T_f$ , and in saline water the opposite is true. Even though brackish water has a maximum density above the freezing point, the maximum is weaker the larger is the salinity (Fig. 2.4b). In freshwater lakes, the freezing point is between  $-0.03$  and  $0^\circ\text{C}$ , and the temperature of maximum density is between  $3.87$  and  $3.98^\circ\text{C}$ .

Linear approximations of Eq. (2.7a, b) are:

$$T_m = 3.98 - 0.223 \cdot S - 0.0207 \cdot p \quad (2.8a)$$

$$T_f = -0.0549 \cdot S - 7.53 \times 10^{-3} \cdot p \quad (2.8b)$$

The pressure term in Eq. (2.8a) is a linear fit to the outcome from the equation of state, exact at  $p = 0$  and  $100$  bar, showing that the temperature of maximum density decreases with increasing pressure by about  $0.1^\circ\text{C}/5$  bar. The freezing point is exact at  $p = 0$ ,  $S = 0$  and  $S = 35$  ‰.

**Example 2.3.** Lake Baikal is a deep, freezing fresh water lake in Siberia. At 1-km depth, the temperature of maximum density is  $1.91^\circ\text{C}$ , and at this temperature and depth the density of water is  $1004.9 \text{ kg m}^{-3}$ . The freezing point is  $-0.75^\circ\text{C}$  at this depth. The subglacial Lake Vostok is beneath the Antarctic ice sheet. The pressure is of the order of  $350$  bar (Siegert et al. 2001), and, consequently, if the water is fresh, then  $T_f = -2.64^\circ\text{C}$  and  $T_m = -3.95^\circ\text{C}$ .

In hypersaline waters, the freezing point depends more strongly on the chemical composition of the dissolved substances. At high salinities, the freezing point depression is no more linear, and different salts crystallize at their individual eutectic temperatures

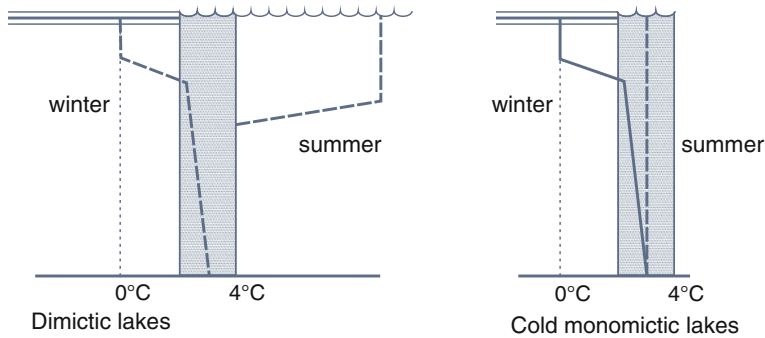


**Fig. 2.5** Temperature stratification in dimictic and cold monomictic lakes. The *dotted rectangle* denotes for autumn and spring overturn of the water mass

(for seawater, see Assur 1958). Therefore the freezing point formula is more clearly lake-specific. The Great Salt Lake of Utah does not freeze although there is snow around in winter. Also it is well known that Don Juan Pond with the salinity 440 ‰ in Antarctica does not freeze at  $-50^{\circ}\text{C}$  during the austral winter (Meyer et al. 1962).

Unstable density stratification does not hold in natural conditions, and therefore increase of surface water density leads to convective mixing. The temperature of maximum density of fresh water is close to  $4^{\circ}\text{C}$ , and when the surface temperature reaches this level, the whole water column is mixed by vertical convection. This is also called the *water mass turnover*. The oxygen storage of fresh water lakes is renewed in turnover events, which are necessary for aquatic life.

In the response of freshwater lakes to thermal forcing, overturn events are crucial. This event is especially strong in the cooling season, starting from the deepening of the mixed layer in the autumn. Convective mixing deepens until the surface water temperature reaches the temperature of maximum density, and then mixing can continue by wind forcing to lower temperatures. The water temperature lags behind the air temperature forcing with the ‘thermal memory’ depending on the lake depth. For shallow lakes the memory is less than 1 month, and for deep lakes it can be several months. Water volumes are fairly small, but if the annual cycle is strong, lakes may store much heat in the summertime to be released in winter. Summer heat is also stored in the bottom sediments in shallow lakes.

The annual frequency of the turnover events is the basis of *limnological classification* of lakes (Fig. 2.5). Most seasonally freezing lakes have two turnover events—in spring and fall—and thus are *dimictic*. The summer stratification<sup>3</sup> shows warm upper layer and cold lower layer with a thermocline layer between, where the temperature changes sharply. In winter, the stratification is inversed. However, the time between spring and fall mixing becomes shorter with colder climate, and when cold enough they merge together

<sup>3</sup> In limnology the upper layer is called epilimnion and the lower layer is called hypolimnion.

—the lakes are then cold *monomictic*. Lake with perennial ice can be *polymictic* or *amictic*, but if they are completely ice-covered the oxygen storage is not renewed.

In shallow brackish, saline or hypersaline lakes, wind-driven or wave-driven mixing can drive the turnover. But in deep lakes, vertical mechanical mixing may be limited, and permanent salinity stratification develops. The layer with a sharp change in salinity is called a *halocline*, analogous to the thermocline. If the halocline is very weak, the bottom water may be renewed locally by increase of salinity due to evaporation or salt rejection in freezing. If this is not the case, the lake is classified as *meromictic*, referring to the existence of a lower layer of water, which does not intermix and hence is anoxic. In principle, ventilation of such layer could take place by inflow of more saline water, but that is possible only in particular environmental conditions. Example in Finland there are small meromictic lakes, where the stratification has developed after the Last Ice Age.

**Example 2.4.** Consider a cold lake with temperature  $T_b$  and salinity  $S_b$  in the lower layer and salinity  $S_0 < S_b$  in the upper layer. Vertical ventilation of the water body is possible, if  $\rho(T_m, S_0) > \rho(T_b, S_b)$ . This can be exactly solved from the equation of state (Eq. 2.4), but a first-order approximation can be made using Eq. (2.5) with a salinity term  $\beta \cdot S_b$ ,  $\beta \sim 0.8 \text{ kg m}^{-3}$  added. Then we can obtain the ventilation condition (salinity in ‰):

$$S_b - S_0 < \frac{\alpha}{\beta} [T_b - T_m(S_b)]^2$$

Since  $\alpha/\beta \sim 10^{-2} \text{ }^\circ\text{C}^{-2}$ , it is seen that for  $T_b - T_m(S_b) = 3 \text{ }^\circ\text{C}$ , we must have  $S_b - S_0 < 0.1 \text{ ‰}$ .

The temperature pair of the maximum density and the freezing point ( $T_m, T_f$ ) is the basis of the classification of the cooling process in lakes. In fresh and brackish lakes, as soon as  $T_0 < T_m$ , the lake is potentially capable to freeze, because then the density decreases in cooling, and in calm conditions only a short, cold period may result in a thin ice cover. Kirillin et al. (2012) called ‘pre-winter’ the period, when the surface temperature is below  $T_m$  and the surface is still ice-free. The condition  $T_0 \leq \max(T_m, T_f)$  means always a risk of ice formation. However, the strength of the inverse stratification becomes weaker with increasing salinity (Fig. 2.4b). In saline and hypersaline lakes, the potential freezing condition comes only when the surface temperature has reached the freezing point. Lakes can be classified for the ice season (see also Fig. 2.2) into (Table 2.4).

Proglacial lakes form a special group of ice-covered lakes. They form in front (epiglacial lakes), on top (supraglacial lakes) or underneath (subglacial lakes) of glaciers and ice sheets, and glacial melt water is their main water source (Menzies 1995). Epiglacial lakes have normally a seasonal ice cover, and they are much as normal cold region lakes. Supraglacial lakes have seasonal or perennial ice cover and the body is in liquid state usually in summer only (e.g., Leppäranta et al. 2013). Subglacial lakes have a perennial, glacial ice cover, and they are usually under a heavy pressure caused by the thick ice.

**Table 2.4** Classification of lakes according to the quality of the ice season

Ice cover	Explanation	Surface temperature $T_0$	Limnological type
Ephemeral	Ice formation possible	Winter $T_0 \leq \max(T_m, T_f)$	DM, MM
Seasonal	Ice forms and melts	Winter $T_0 = T_f$	DM, CM, PM, MM
Perennial	Multi-year ice	Summer $T_0 \approx T_f$	CM, AM, PM, MM

DM Dimictic; CM Cold monomictic; PM Polymictic; AM Amictic; MM Meromictic

Physical properties of fresh water can be taken constants for many applications (Table 2.5). Temperature, salinity and pressure modify the physical properties of water, but apart from electromagnetic properties the influence is small. The density is, however, an important exception, since beneath the ice cover very small differences have a major role in the circulation of lake water masses. Very high pressure, or equivalently great depth, needs to be considered in subglacial lakes and cooling of very deep lakes. In the other extreme, at the surface of high mountain lakes the pressure is low that has influence primarily on the saturation levels of dissolved gases.

*Optical classification* of lake waters goes for the colour and transparency (Arst 2003; Arst et al. 2008). Coloured dissolved organic matter (CDOM), suspended matter, and chlorophyll *a* are the basis of this classification. The strength of brown colour is related to the concentration of CDOM, while turbidity is related to the concentration of suspended matter. Because humic substances give a large contribution to CDOM in boreal lakes, in classical limnology, the colour of water is given by the degree of brown colour in filtered water samples, obtained by comparing the water sample colour with the colour of platinum

**Table 2.5** Physical properties of fresh water ( $S < 0.5$  ‰) at the temperature of 0 °C and comments on the variability of these properties in cold water. Standard atmospheric pressure is assumed

Property	Value ( $T = 0$ °C, $S = 0$ )	Variability
Molecular weight	$18.02 \text{ g mol}^{-1}$	–
Density	$1,000 \text{ kg m}^{-3}$	Equation of state
Thermal expansion	$-6.7 \times 10^{-5}$	$\rightarrow 0$ at 3.98 °C, $>0$ at higher $T$
Viscosity	$1.79 \times 10^{-3} \text{ N s m}^{-1}$	$1.57 \times 10^{-3} \text{ N s m}^{-1}$ at 4 °C
Surface tension	$75.6 \text{ N m}^{-1}$	$<1$ % ( $75.1 \text{ N m}^{-1}$ at 4 °C)
Compressibility	$0.51 \times 10^{-10} \text{ Pa}^{-1}$	Very small
Speed of sound	$1,402 \text{ m s}^{-1}$	$1,421 \text{ m s}^{-1}$ at 4 °C
Specific heat	$4.22 \text{ kJ kg}^{-1} \text{ °C}^{-1}$	$<1$ %
Thermal conductivity	$0.561 \text{ W m}^{-1} \text{ °C}^{-1}$	$\approx 1$ %
Latent heat of freezing	$333.5 \text{ kJ kg}^{-1}$	–
Latent heat of evaporation	$2.49 \text{ MJ kg}^{-1}$	$<1$ %
Electric conductivity	$<1 \text{ } \mu\text{S cm}^{-1}$	Highly sensitive to salinity <sup>a</sup>
Relative permittivity	87.9	Sensitive to salinity

<sup>a</sup>In pure water the electric conductivity is extremely small but then rises fast with salinity

**Table 2.6** Lake classification systems

Background	Object	Basis
Geological	Lake basin	Origin of the depression where the lake has formed
Physical	Size	Horizontal extent and depth
Geochemical	Salinity	Influence on water density and other properties
Limnological	Mixing	Frequency of convective overturn of the water mass
Optical	Colour	Optically active substances
Biological	Trophic status	Level of nutrients
Cryospheric	Ice	Quality of ice season

solutions (the unit is mg Pt, which refers to the concentration of dissolved platinum). Generally, in clear lake waters the Secchi depth<sup>4</sup> is more than 5 m, while it is less than 1 m in strongly brown, turbid or eutrophic water. The *optical thickness* of lake water, defined as the e-folding distance of light intensity, provides the scale for the mixing depth in calm waters due to solar heating.

The *biological classification* is based on the trophic status. This contains the *ultra-oligotrophic*, *oligotrophic*, *mesotrophic*, *eutrophic*, and *hyper-eutrophic* categories. The trophic status is related to the concentrations of phosphorus and nitrogen, that is reflected in the optical quality of the water. Therefore the response of a water body to the ice period depends on the trophic status. Consumption of oxygen is much faster in eutrophic or hyper-eutrophic lakes and they reach more easily anoxic conditions in winter.

A summary of the lake classification systems is given in Table 2.6. There have been approaches to classify the size of lakes on the basis of physical processes. Example the background can be the Coriolis acceleration, which leads to the use of the Rossby radius of deformation as the size criterion (Kirillin et al. 2012). Ashton (1980) classified freezing lakes into small lakes (lakes with stable ice cover), reservoirs (stable ice cover and significant through flow), and large lakes (lakes with drift ice).

---

## 2.2 Weather and Climate

### 2.2.1 General Regional Climate

The local climatology determines to a large degree whether a lake freezes over or not. However, geothermal, hypersaline, and very deep lakes are able to stay ice-free in cold winters. The world’s climate conditions are classified according to the Köppen–Geiger

---

<sup>4</sup> Secchi depth is the maximum depth where a white disk, diameter 30 cm, is visible from the surface.



system into five main classes depending on the temperature  $T$  and precipitation  $P$  (Fig. 2.6):

A Equatorial climates	$T_{\min} > 18\text{ }^{\circ}\text{C}$
B Arid climates	Threshold depends on $T_{\text{mean}}$ and $P$
C Warm temperate climates	$-3\text{ }^{\circ}\text{C} < T_{\min} < 18\text{ }^{\circ}\text{C}$
D Snow climates	$T_{\min} < -3\text{ }^{\circ}\text{C}$
E Polar climates	$T_{\text{max}} < 10\text{ }^{\circ}\text{C}$

There are further subclasses based on temperature and precipitation criteria. It is clear that freezing lakes are found in snow climates and polar climates. Also, there are cold regions in the arid climate zone, and at the cold boundary of the warm climate zone lakes may freeze in some winters. Thus climatic conditions have a very large variability across the zones where lakes freeze. Apart from very large lakes, the size of lakes is small compared to weather systems, and therefore the atmospheric conditions over a given lake are fairly homogeneous. However, more variability may be seen in the drainage basins, which are often much larger than the lake where the water is collected.

Large-scale weather systems are described by various indexes based on the atmospheric pressure distribution. In Europe, widely used is the NAO (North Atlantic Oscillation) index, which tells of the intensity of the westerlies. In exact terms, NAO equals the

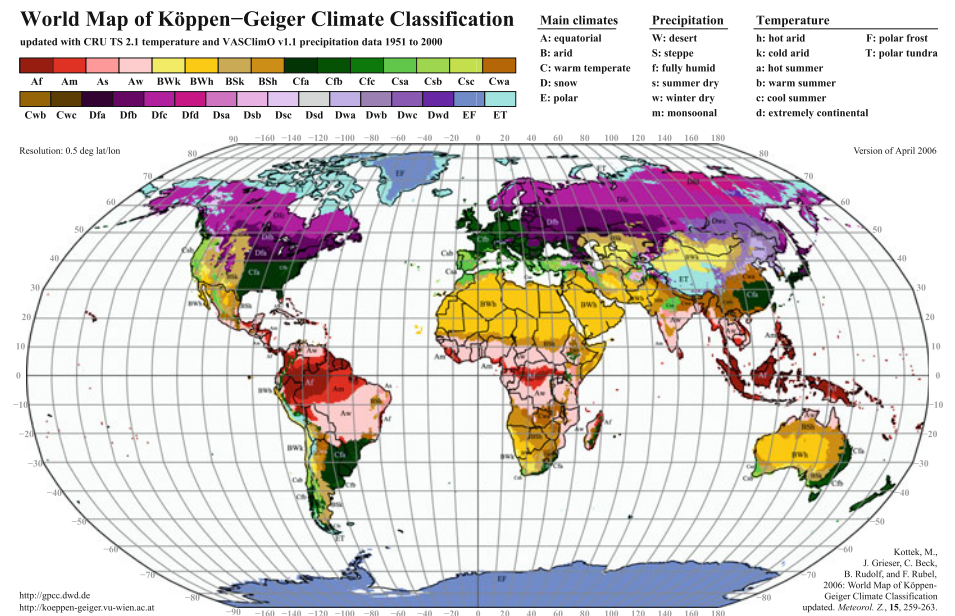


Fig. 2.6 Köppen-Geiger classification of climates (Kottek et al. 2006)

normalized anomaly of the difference in the heights of the 500 mbar atmospheric pressure surfaces between the Azores (Ponta Delgada) and Iceland (Stykkisholmur). The NAO-index is positive, when the westerly winds are stronger than normal and these winters in Europe are typically much warmer than on average; when the NAO-index is negative, the westerlies are weaker and the winters are cold. The index value 1 (−1) means that the westerly winds at 500 mbar level between Iceland and the Azores are one standard deviation stronger (weaker) than on average. Much of the variability of lake ice seasons in Europe is correlated with NAO. This is trivial but it is noteworthy that the correlation is quite high and therefore general regional climate overcomes the individual characteristics of lakes (e.g., Blenckner et al. 2004). In land regions around the Pacific Ocean, El Niño–Southern Oscillation (ENSO) is connected to anomalously warm and cold winters (e.g., Mishra et al. 2011).

The influence of weather and climate on frozen lakes is by the exchange of mass, heat and momentum between lakes and atmosphere and solar radiation. These fluxes between the atmosphere and lakes depend on the precipitation, air pressure, cloudiness, air temperature and humidity, and wind. The standard weather station data include air pressure, temperature and humidity at 2 m altitude, and wind speed and direction at 10 m altitude; some stations also provide cloudiness. Since direct measurements of solar and terrestrial radiation components are rarely available, cloudiness becomes a key variable for their indirect estimation. Table 2.7 presents climatological data from stations Jokioinen (snow climate, boreal zone) and Utsjoki (polar climate, tundra zone).

The atmospheric mass flux to a lake is given by the difference between precipitation and evaporation/sublimation. Precipitation is obtained directly from weather observations, but evaporation and sublimation need to be estimated using atmospheric boundary layer and surface temperature data.

Absolute humidity is given by the mass proportion of water vapour ( $q$ ) or by the partial atmospheric pressure due to water vapour ( $e$ ). They are related by

$$q = 0.622 \frac{e}{p} \quad (2.9)$$

The maximum amount of water vapour depends strongly on the temperature (Fig. 2.7; for the exact formulae, see Annex); at temperatures below zero, the saturation level is given both for liquid water surface and for ice surface. Example the saturation water vapour pressure at the standard atmospheric pressure is 12.27 mbar at the temperature of 10 °C, 6.11 mbar at 0 °C, and 2.86 mbar (water surface) or 2.60 mbar (ice surface) at −10 °C. The relative humidity is the actual humidity in relation to the saturation value:

$$R = \frac{q}{q_s} = \frac{e}{e_s} \quad (2.10)$$

**Table 2.7** Climatological data from the normal period 1981–2010 for Jokioinen (60°48'N 23°30'E) and Utsjoki Kevo (69°45'N 27°00'E)

Jokioinen	Temperature (°C)	Precipitation (mm)	Incoming solar radiation (W m <sup>-2</sup> )	Relative humidity (%)	Cloudiness (1/8)	Wind	
						m/s	direction
January	−5.6	46	11	89	6.4	3.6	165
February	−6.3	32	38	87	6.0	3.5	171
March	−2.4	32	87	82	5.5	3.5	168
April	3.5	30	152	72	5.6	3.5	153
May	9.8	41	208	65	5.1	3.5	163
June	14.0	63	225	68	4.9	3.3	235
July	16.7	75	218	71	5.3	3.1	201
August	15.0	80	162	77	5.6	3.1	150
September	9.9	58	97	83	5.9	3.3	194
October	4.9	66	41	88	6.2	3.5	194
November	−0.2	57	13	91	6.7	3.7	164
December	−3.9	47	6	91	6.6	3.7	173

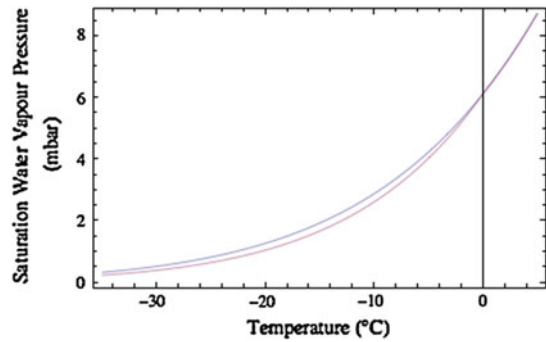
Utsjoki	Temperature (°C)	Precipitation (mm)	Incoming solar radiation (W m <sup>-2</sup> )	Relative humidity (%)	Wind	
					m/s	direction
January	−14.0	27	1	85	2.8	165
February	−12.8	24	15	83	2.9	171
March	−8.2	21	66	81	3.0	168
April	−2.5	25	146	76	2.9	153
May	3.7	27	181	72	3.0	163
June	9.6	50	195	68	3.2	235
July	13.1	72	170	74	2.9	201
August	10.7	57	116	80	2.6	150
September	5.7	38	61	85	2.6	194
October	−0.5	39	29	88	2.7	194
November	−8.3	28	1	88	2.6	164
December	−12.3	25	0	86	3.7	173

The data are from Pirinen et al. (2012) except cloudiness is from 1971–1980 (FMI 1982)

where  $q_s$  and  $e_s$  are the saturation levels of specific humidity and water vapour pressure, respectively. Annual variations in relative humidity are usually small, but the absolute humidity follows largely the air temperature.

Solar radiation has a strong annual cycle in high-latitude lakes, so that the radiation balance is switched from positive to negative for the cold season. It reflects the presence of polar summer and polar winter in the north. Over lakes, the sensible and latent heat losses to the atmosphere are strong in fall and winter as long as the surface is ice-free but go down after the ice has formed. Transport of warm air from lower latitudes by intensive cyclone activity may delay ice formation. This transport is especially strong for central and northern Europe since the North Atlantic Current brings warm water and adds heat into the atmosphere. When the westerlies are strong (positive NAO index), they are able to transport this oceanic heat to lakes in the European continent.

**Fig. 2.7** Saturation water vapour pressure as a function of temperature at water surface, and at ice surface



Momentum, heat and moisture transfer between lakes and atmosphere are determined by atmospheric boundary layer processes. Wind velocity gives the momentum transfer in terms of the tangential surface stress, and to estimate the drag properly, temperature and humidity distributions are also needed to account for the stability of the atmospheric surface layer. True weather data over lakes can be obtained from floats (Fig. 2.8). Routine weather stations are located on land, and using their data for the lake surface needs particular consideration.

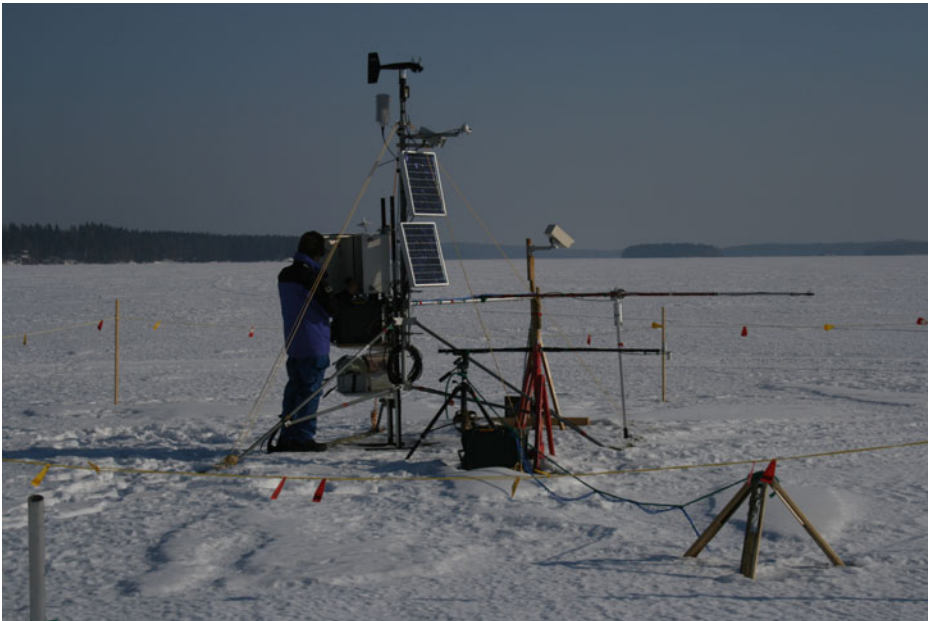


**Fig. 2.8** Ice station *Lotus*, Lake Pääjärvi in southern Finland (e.g., Wang et al. 2005; Jakkila et al. 2009). Solar power panels and atmospheric surface layer instrumentation is seen *above* the lake surface. Also included are the instrumentations for ice (temperature and light) and water body (temperature, light, conductivity, flow velocity)

### 2.2.2 Air Pressure

The influence of air pressure in lake physics steps in primarily by its influence on the physical properties of air across large altitudinal differences. Also horizontal air pressure variations may induce seiches in ice-covered lakes (Kirillin et al. 2012). At the sea surface level, air pressure is within 900 and 1,100 mbar, while the standard atmospheric pressure is 1013.25 mbar. In weather station records, the atmospheric pressure is normally reduced to the sea surface level.

By the hydrostatic law (Eq. 2.5), air pressure decreases with height. Since air is compressible, the pressure–height relation is a little complicated. With decreasing pressure, temperature and density also decrease. The equation of state for dry air is  $p = \rho R_d T$ , where  $R_d = 287 \text{ J K}^{-1} \text{ kg}^{-1}$  is the gas constant of dry air. Then the temperature decreases with pressure and follows the dry adiabatic lapse rate

$$\Gamma = \frac{g}{c_{pd}(1 + 0.87q)} \quad (2.11)$$

where  $c_{pd} = 1,004 \text{ J K}^{-1} \text{ kg}^{-1}$  is the specific heat of dry air at constant pressure, and  $q$  is the specific humidity. For  $q = 0$ ,  $\Gamma = 9.8 \text{ K km}^{-1}$ . In air saturated with water vapour, the lapse rate is less, because condensation releases heat to partly compensate for the influence of pressure release. In the troposphere, the normal adiabatic lapse rate is  $\Gamma = 6.5 \text{ K km}^{-1}$  (e.g., Holton 1979; Curry and Webster 1999). The pressure distribution is given by:

$$p(z) = p(0) \left( 1 - \frac{\Gamma}{T_0} z \right)^{\frac{g}{R_d \Gamma}} \quad (2.12)$$

where  $T_0$  is the surface temperature. The power in Eq. (2.12) is 5.25 for  $\Gamma = 6.5 \text{ K km}^{-1}$ . In mountain lakes the ambient pressure needs to be accounted for the surface conditions. The primary influence of the reduced pressure goes in the solubility of gases into water.

**Example 2.5.** Equation (2.12) tells that in the troposphere the pressure decreases by about 100 mbar/1 km increase in elevation. Thus at 5 km altitude the air pressure is around 500 mbar. This equation can be also solved for the height as a function of pressure when the surface temperature and pressure are known. The adiabatic lapse rate provides the temperature decrease with altitude in neutral conditions:  $T(z) = T_0 - \Gamma z$ . At 5 km altitude, the temperature is 32.5 K lower than at the sea surface level. If  $T_0 > T_f$ , the freezing point is reached at the altitude of  $(T_0 - T_f) \cdot \Gamma^{-1}$ .

2.2.3 Precipitation

Precipitation provides the external mass flux to drainage basins. The level of precipitation is connected to atmospheric humidity, temperature and circulation, and orography, since the saturation water vapour pressure is sensitive to temperature (Fig. 2.7). Therefore precipitation is usually lower in colder climate (see Table 2.8). The main exceptions are in the tropics, where descending air masses produce very small amount of precipitation, and at mountains, where orographic effects may force air masses upward and result in heavy precipitation. The highest precipitation levels over ice-covered lakes are observed in mid-latitude mountain areas, e.g. in European Alps, Rocky Mountains in North America, and Japanese Alps, where the annual precipitation is 2,000–3,000 mm. Toward the polar regions, the precipitation level decreases, and as an extreme case, there is no precipitation in Antarctic dry valleys.

Precipitation data are available from most weather stations. It is given in terms of accumulation rate of an equivalent liquid water layer, normally in millimetres per time. Precipitation gauges are used for the measurements. There are large difficulties to determine the solid precipitation, especially during snowstorms due to turbulent transport of snowflakes, and the recorded snow accumulation data are often biased down. Instead of simple cylindrical gauges, in cold climate regions precipitation gauges are equipped with specific structures to manage the snowfall aerodynamics properly (Fig. 2.9).

In cloud altitudes the air temperature is typically below the freezing point due to adiabatic cooling. Because the saturation water vapour pressure is lower at ice surface than at water surface (Fig. 2.7), deposition of water vapour into ice crystals is more likely than condensation into water droplets. If the atmosphere is cold down to the Earth’s surface, precipitation lands in the solid phase. Hailstones fall fast and can reach the ground even in warm conditions. The shape of the falling ice or snow crystals depends on the temperature and the degree of oversaturation in clouds (Fig. 2.10). If the phase of precipitation is unknown, a practical approach is to take it solid when the air temperature is below a specified level, e.g. below  $-1\text{ }^{\circ}\text{C}$ .

**Table 2.8** Quality of ice season in different cold climate zones

	$P(I) = 0$	$0 < P(I) < 1$	$P(I) = 1$
$P(O) = 0$	X	X	Perennial
$0 < P(O) < 1$	X	Perennial/seasonal/ephemeral	Perennial/seasonal
$P(O) = 1$	Ice free	Ephemeral	Seasonal

P(I) and P(O) are the probabilities of the annual occurrences of ice and open lake, respectively; X stands for ‘not possible’





**Fig. 2.9** Tretyakov model precipitation gauge with a snowfall capture system (*left side*). The metal slices around the cylinder constitute the specific design for aerodynamics to obtain good snowfall data. On the right, an old gauge behind the cabled box

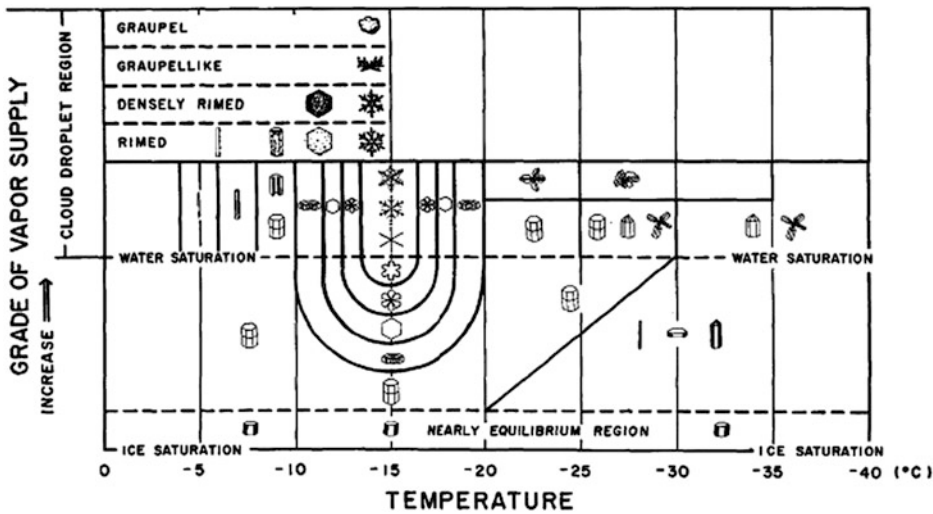


**Fig. 2.10** Snow crystal structure as a function of temperature and oversaturation (modified from Magano and Lee 1966)

### 2.2.4 Air Temperature, Humidity and Wind

Air temperature is a widely used characteristic in geoscience and ecology. It is a quite stable quantity, its measurement is easy to perform and can be made accurately, and there are long-term data available for<sup>5</sup> many observation stations around the world. Humidity is normally expressed as the relative humidity, and it is a key factor in evaporation/condensation and sublimation/deposition, which are important in the mass and heat budgets of lakes. Temperature and humidity are recorded in all weather stations, and their reference altitude has been defined as 2 m above the surface. Wind, measured in most weather stations, refers to two-dimensional, horizontal airflow and is expressed by its speed and direction at the standard altitude of 10 m above the surface.<sup>6</sup>

The annual cycle of the air temperature largely follows the solar radiation (Table 2.7). In summer, the Sun and warm air heat lakes and the surface temperature reaches maximum, while in fall the situation is reversed, as lake waters are warmer than the cooling atmosphere. In general, the amplitude of the annual cycle of air temperature is larger in land areas than in lake districts. Apart from geothermal and deep lakes, the difference between the air temperature and surface temperature is small except for transient events. Thus, for a lake to freeze, in practice the air temperature cannot be much above the freezing point. As long as the drainage basin is snow-covered, the air temperature can be significantly above 0 °C only due to advection of warm air.

In cold climate the absolute humidity of air is small, and therefore mass and heat fluxes due to evaporation/sublimation or condensation/deposition are much smaller than in warm climate, order of 1 mm water equivalent<sup>7</sup> per day. But due to the large latent heat of phase transitions of water, these fluxes are always significant in the heat balance. In dry and cold climate regions, also mass losses due to sublimation can be significant. Deposition of water vapour onto ice surface is sometimes observed as beautiful ‘frost flowers’. However, it takes place rarely so that it is insignificant in the heat and mass balance.

Wind velocity shows large local and regional variations depending on the surface topography, vegetation and stratification of the atmospheric surface layer. Therefore wind velocity is sensitive to local conditions at an observation station, and the difference in wind between a lake and nearby land station can be large. Sometimes correction factors are employed to estimate the wind velocity on a lake from land station measurements.

---

<sup>5</sup> Celcius (°C) is a convenient temperature unit in investigations of freezing lakes and mostly used in this book. The absolute temperature (Kelvin) is the natural scale for thermodynamics and used here where considered preferable. These units transform by  $273.15 \text{ K} = 0 \text{ °C}$ .

<sup>6</sup> Wind direction (WD, degrees) tells from where the wind blows in the compass angle, zero toward north and turning clockwise. Mathematical right-hand coordinate system has zero direction toward east (x-axis) and turns counter-clockwise. Wind vector direction (to where the wind blows) is in the right-hand system  $270^\circ - \text{WD}$ .

<sup>7</sup> Water equivalent refers to the thickness of a layer of liquid water with corresponding volume.

Air temperature, humidity and wind speed determine the turbulent transfer of momentum, heat and moisture between the atmosphere and lakes. The bulk formulae to estimate these fluxes are, respectively,

$$\tau_a = \rho_a C_a U_a U_a \quad (2.13a)$$

$$Q_c = \rho_a c_p C_H (T_a - T_0) U_a \quad (2.13b)$$

$$Q_e = \rho_a L^* C_e (q_a - q_0) U_a \quad (2.13c)$$

where  $\rho_a$  is the air density,  $C_a$ ,  $C_H$  and  $C_E$  are the bulk exchange coefficients for momentum, heat and moisture, and  $L^*$  is the latent heat of evaporation ( $L^* = L_e$ ) or latent heat of sublimation ( $L^* = L_f + L_e$ ) depending on the quality of the moisture transfer, and  $U_a$  is the wind speed. We can assume that the humidity is at the saturation level at the surface,  $q_0 = q_s(T_0)$ . The magnitude of the turbulent exchange coefficients is  $10^{-3}$ , and in general they depend on the surface roughness and stratification of the atmospheric surface boundary layer (see Sect. 4.1.4 for more details). In the neutral case,  $1.2 \times 10^{-3}$  is a good reference value (Andreas 1998). Example for the wind speed of  $5 \text{ m s}^{-1}$ , the momentum transfer is  $0.039 \text{ Pa}$ , the sensible heat exchange is  $7.8 \text{ W m}^{-2}/1^\circ\text{C}$  temperature difference between air and the surface, and the latent heat exchange is  $12.1 \text{ W m}^{-2}$  (evaporation/condensation) or  $13.7 \text{ W m}^{-2}$  (sublimation/deposition) per 1 mbar difference in the water vapour pressure.

The characteristics of the atmospheric surface boundary layer have a clear seasonal dependence. In autumn, lakes are usually warmer than the air, and the boundary layer is unstable. Then the turbulent fluxes are strong. In spring and early summer the air is warmer than lake surface, the boundary layer is stable and winds usually remain weak, and, consequently, turbulent transfer is weak. Routine weather station observations provide the atmospheric information needed to evaluate the air–lake interaction except for the surface temperature.

### 2.2.5 Radiation Balance

The radiation balance consists of solar and terrestrial radiation, and the net radiation provides the governing forcing to the annual course of the freezing lakes. The physical basis is the Planck's law of black body radiation, which provides the distribution of thermal radiation as a function of temperature and wavelength. When this law is integrated over the wavelengths, we have the *Stefan-Boltzmann law*, which tells that the radiative heat flux is proportional to the fourth power of the absolute temperature. Natural objects radiate a little less than a black body; if the spectral distribution of radiation is similar to the black body law, the object is called a *grey body*. The radiative flux of a grey body

equals the radiative flux of a black body, at the same temperature, multiplied by its emissivity  $\varepsilon$  ( $0 \leq \varepsilon \leq 1$ ):

$$Q = \varepsilon \sigma T_0^4 \quad (2.14)$$

where  $\sigma = 5.6704 \times 10^{-8} \text{ W m}^{-2} \text{ K}^{-4}$  is the Stefan-Boltzmann constant, and  $T_0$  is the surface temperature. The black body case comes with  $\varepsilon = 1$  in Eq. (2.14). Sun and lake surface (whether liquid water, ice or snow) radiate almost as black bodies ( $\varepsilon > 0.95$ ). For a grey body, the *radiative temperature*  $T_R$  is defined from  $\sigma T_R^4 = \varepsilon \sigma T_0^4$ .

The *solar constant* is defined as the annual average of solar radiation incident on a plane perpendicular to the solar rays on the top of the atmosphere. Its value is equal to  $1367 \text{ W m}^{-2}$  (e.g., Iqbal 1983). On the way through the atmosphere, this radiation is reduced by 30–80 % due to absorption and scattering. Solar radiation makes a strong seasonal cycle over freezing lakes (Table 2.7). Part of the *incoming solar radiation* is reflected and scattered back at the lake surface, called as the *outgoing solar radiation*. The ratio of outgoing to incoming radiation is the *albedo* ( $\alpha, 0 \leq \alpha \leq 1$ ), which has a very important role during the lake ice season, in particular in the melting period.

Incoming and outgoing solar radiation are in exact terms downwelling and upwelling, respectively, planar *irradiances* at the surface (see, e.g., Arst 2003). These irradiances integrate the radiance coming from a hemisphere onto a horizontal plane element. Downwelling and upwelling solar irradiances<sup>8</sup> are measured directly by using a pyranometer. Only few weather stations provide direct measurements of solar radiation on a routine basis but simple formulae are available to estimate it using routine weather data (see Sect. 3.4.1).

In terrestrial radiation, lake surface acts as a grey body with emissivity  $\varepsilon_0$  in the range 0.96–0.98. For  $\varepsilon_0 = 0.97$ , the emitted thermal radiation is  $306 \text{ W m}^{-2}$  at  $0^\circ \text{C}$  (the range is  $303\text{--}309 \text{ W m}^{-2}$  for  $\varepsilon_0 = 0.96\text{--}0.98$ ), and for the temperature range from  $-20$  to  $20^\circ \text{C}$  the emitted radiation varies through  $226\text{--}406 \text{ W m}^{-2}$ . Thermal radiation from the atmosphere is more complicated since it comes from atmospheric gas molecules, aerosols, water vapour, water droplets and ice crystals, from different altitudes with different temperatures. An analogous formula to grey body radiation, for parameterization from normal weather data, is used with ‘effective emissivity’ and the surface air temperature (altitude 2 m) as the representative temperature. This effective emissivity is  $\varepsilon_a = 0.7\text{--}0.9$ , giving the radiation at  $0^\circ \text{C}$  in the range of  $221\text{--}284 \text{ W m}^{-2}$ , and, consequently, the net terrestrial radiation is then negative.

Terrestrial radiation can be measured with pyrgeometers, but such data are not available in routine weather records. To estimate the atmospheric thermal radiation is a key problem in the heat balance evaluation since indirect estimates based on the routine weather data are not so accurate. Cloudiness is the key factor, which is available at some weather stations but good data are coming less and less as they are produced only by

<sup>8</sup> The total downwelling solar irradiance on a horizontal plane is also called *global radiation*.

visual observations of trained personnel. Secondary influence on the radiation level is due to water vapour, other greenhouse gases, and aerosols.

In the polar zone, sunlight is absent in mid-winter, while in the polar summer the daily maximums of solar radiation become up to  $500\text{--}800 \text{ W m}^{-2}$ . Albedo of open water, ice and snow are of the order of 0.1, 0.5 and 0.9, respectively, and therefore the quality of the surface makes a major contribution to the net solar radiation absorbed by a lake: the net daily maximum is  $50\text{--}500 \text{ W m}^{-2}$ . The net terrestrial radiation

$$Q_{\text{nL}} = \varepsilon_0 \sigma (\varepsilon_a T_a^4 - T_0^4) = \varepsilon_0 \sigma (T_{\text{Ra}}^4 - T_0^4) \quad (2.15)$$

is of the order of  $-50 \text{ W m}^{-2}$ . It is in practice always negative and varies during the annual cycle mostly from  $-20$  to  $-80 \text{ W m}^{-2}$ . The wavelength band of solar radiation is in practice  $0.3\text{--}3 \mu\text{m}$ , while the terrestrial radiation band is  $5\text{--}15 \mu\text{m}$ . This is why they are also called short-wave and long-wave radiation, respectively.

**Example 2.6.** A simple planetary climate model (no atmosphere) is based on the balance between the net solar radiation and the emitted terrestrial radiation from the surface. The balance and the solution are:

$$\varepsilon_0 \sigma T_0^4 = \frac{1}{4} \cdot (1 - \alpha) Q_{\text{sc}} \text{ or } T_0 = 4 \sqrt{\frac{(1 - \alpha) Q_{\text{sc}}}{4 \varepsilon_0 \sigma}}$$

where the factor  $1/4$  comes from averaging the solar radiation over the planet. The planetary albedo of the Earth is 0.3, and taking  $\varepsilon_0 = 0.97$ , we have  $T_0 = -16^\circ\text{C}$ . For other planets, the albedo can be different and the ‘solar constant’ is inversely proportional to the square of the distance between the planet and the Sun.

We can extend this model by adding atmosphere, with emissivity  $\varepsilon_a$ , and letting the solar radiation be absorbed at the surface ( $b_0$ ) and in the atmosphere ( $b_1$ ),  $b_0 + b_1 = 1 - \alpha$ . Then we have a pair of equations for the temperatures at the surface and in the atmosphere, and the surface temperature becomes:

$$T_0 = 4 \sqrt{\frac{b_0 + \frac{1}{2} \varepsilon_0 b_1}{(1 - \frac{1}{2} \varepsilon_0 \varepsilon_a)(b_0 + b_1)}} \cdot \frac{(1 - \alpha) Q_{\text{sc}}}{4 \varepsilon_0 \sigma}$$

where the factor  $1/2$  comes from the atmosphere losing heat by radiation to its both sides. On the right-hand side, the first factor constitutes the atmospheric correction, and the second factor is the no-atmosphere solution. Taking  $\varepsilon_a = 0.8$ ,  $b_0 = 0.65$  and  $b_1 = 0.05$ , corresponding to planetary albedo of 0.3, we have  $T_0 = 12.6^\circ\text{C}$ , which is not far from the present global average (about  $15^\circ\text{C}$ ). It is clear that the result is sensitive to the atmospheric emissivity and albedo.

**Example 2.7.** In the tropical zone, in the coldest month  $T_a = 300$  K. Taking the adiabatic lapse rate as  $\Gamma = 6.5 \text{ K km}^{-1}$ , the air temperature reaches the freezing point at the altitude of 4.1 km. For the scaling magnitude, we can take  $Q_s \propto \cos Z_0 \times t_{\text{day}}$ , where  $Z_0$  is the solar zenith angle at noon and  $t_{\text{day}}$  is the length of the day. In the northern hemisphere mid-winter, we have approximately  $Q_s = Q_{s0} \times \cos(\phi - \delta)$ ,  $\phi - \delta \leq 90^\circ$ , where  $Q_{s0}$  is the scale of radiation in the tropics,  $\phi$  is latitude, and  $\delta \sim -15^\circ$  is declination. Assuming  $T_0 = T_a$ , the surface temperature is obtained from the radiation balance as

$$T_0^4(\phi) = \frac{(1 - \alpha)Q_{s0}}{\varepsilon_0(1 - \varepsilon_a)\sigma} \cos(\phi - \delta)$$

The temperature decreases with altitude and latitude as  $T_0(z, \phi) = T_0(0, \phi) - \Gamma z$ . We can then solve for  $z = z(\phi)$  where  $T_0(z, \phi) = T_f$  as:

$$z = \frac{1}{\Gamma} \left[ \sqrt[4]{\frac{(1 - \alpha)Q_{s0}}{\varepsilon_0(1 - \varepsilon_a)\sigma} \cos(\phi - \delta)} - T_f \right]$$

The altitude increases towards lower latitudes from zero at  $\phi \sim 40^\circ\text{--}50^\circ$ .

---

## 2.3 Water Budget of Lakes

### 2.3.1 General Form

Lakes are associated with a water budget. The lake water storage  $S$  changes by precipitation ( $P$ ), evaporation/sublimation ( $E$ ), inflow ( $I$ ) and outflow ( $O$ ):

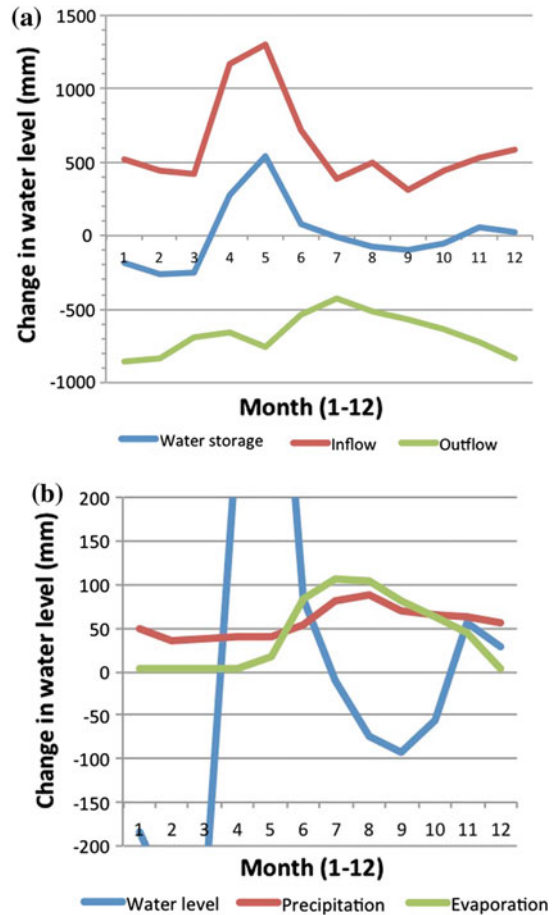
$$\frac{dS}{dt} = (P - E)A + I - O \quad (2.16)$$

where  $A$  is the area of the lake. Inflow and outflow consist of surface and groundwater components. The term  $E$  is normally positive but occasionally, in case of condensation or solid deposition of water vapour, it may appear negative. Sometimes it is desirable to express the storage as  $S = AH$ , where  $H$  is the mean depth. The relative magnitudes of inflow and precipitation are related to the size of the drainage basin of the lake.

The water storage is easy to monitor from the water level elevation, which changes due to the external fluxes. Precipitation is directly measured (Sect. 2.2.3), while evaporation/sublimation can be obtained directly only in special campaigns, and normally it is estimated indirectly from weather station data (Sect. 2.2.4). The most difficult parts are usually the groundwater fluxes and the surface runoff. Figure 2.11 shows an example of the annual course of the water budget in Lake Vanajanselkä, southern Finland. The area of the lake is  $103 \text{ km}^2$ , the mean depth is 7.7 m, and the area of the drainage basin is



**Fig. 2.11** Annual course of the water balance in Lake Vanajanselkä, southern Finland (Jokiniemi 2011): **a** Inflow and outflow; **b** Lake–atmosphere water exchange



2774 km<sup>2</sup>. Due to the large size of the drainage basin, the inflow well dominates over precipitation as the source of water.

The flushing time or the water renewal time of a lake provides one fundamental time scale. This scale is defined as the ratio of volume to input or output:  $t_R = S/(PA + I) = S/(EA + O)$ . In this definition the volume and fluxes represent long-term averages, and to make sense we must have  $dS/dt \approx 0$ . Freezing and melting do not influence the overall water budget but the renewal of the water storage slows down (Fig. 2.12). Freezing of lake water just changes water molecules to the solid state but the water storage is unchanged. And as long as the ice is floating, liquid water level elevation is unchanged.

### Example 2.8.

- (a) Over the annual cycle the net change of water storage is normally close to zero and then  $(P - E) \cdot A = I - O$ . In dry regions,  $P \approx 0$  and  $O = 0$ , and at equilibrium  $AE \approx I$ .



**Fig. 2.12** The water budget of frozen lakes is reduced as compared with open water season. Precipitation is stored in the snow layer, and the ground over large regions is also frozen

(b) The change of the water storage can be written as

$$\frac{dS}{dt} = A \frac{dH}{dt} + H \frac{dA}{dt}$$

Consider a circular lake with a diameter  $L$  and a fixed shore slope  $\beta$  around the lake. Then

$$\frac{1}{A} \frac{dS}{dt} = \left( 1 + \frac{H}{L} \cdot \frac{4}{\tan \beta} \right) \frac{dH}{dt}$$

If the shoreline slope is  $4 \times 10^{-3}$  and  $H/L = 10^{-3}$ , changes in the water storage are equally reflected both in the depth and surface area. The equation can be generalized by changing the factor  $4/\tan \beta$  into a general form  $B = b/\tan \beta^*$ , where  $\beta^*$  is the characteristic slope around the lake and  $b \sim 4$  is a parameter depending on the slope statistics around the lake.

### 2.3.2 Inflow and Outflow

Inflow and outflow consist of surface components and groundwater fluxes. The latter part, which is very difficult to measure directly, can be estimated as the residual of the water balance (Eq. 2.16) when the other terms have been measured. In springs, the inflow is predominantly from the groundwater storage. The source of the inflow is the precipitation over the drainage basin. Outflow is related to the water level elevation in the lake so that the outflow rate increases with increasing elevation.

In the Lake Vanajanselkä case (Fig. 2.11), the inflow and outflow average to  $23.5\text{--}23.8\text{ m}^3\text{ s}^{-1}$ , respectively. These correspond to monthly water layers of 610 and 671 mm spread over the lake surface. The flushing time-scale becomes about 12 months. The inflow shows an annual cycle with peak after snowmelt in April–May, about twice the mean inflow. About 90 % of the inflow comes from River Lepaanvirta, and the contribution of ground water flux is of the order of 1 % of the total. Two minima appear, in March and September. The outflow is much smoother with minimum in summer and maximum in winter largely due to the regulation of the water storage and the outflow is therefore controlled. The change in the water level elevation largely follows the inflow.

The surface inflow comes from the drainage basin along rivers and ditches and as runoff along the land surface. It is low during the ice season since the soil surface layer is usually frozen and precipitation over the drainage basin is mostly solid. Groundwater inflow and outflow also slow down during the cold season. At the time of melting of snow and ice, a major inflow peak follows. Closer to the climatological edge of freezing lakes, liquid precipitation events occur all winter. During the ice season the natural outflow decreases since the surface water level is lowered due to the slow renewal of water. In regulated lakes the water level may be even more depressed if the waters are used for hydropower plants. Water level variations caused by inflow–outflow imbalance have influence on the interaction between ice and shore and ice and lake bottom in the winter season.

### 2.3.3 Lake–Atmosphere Water Fluxes

The atmospheric contribution to the mass balance of lakes is due to precipitation and evaporation/sublimation or condensation/deposition. In general they both tend to decrease toward colder climate conditions since the saturation water vapour pressure in air does so (Fig. 2.7). The net exchange between lake and atmosphere equals  $P - E$ .

In Lake Vanajavesi (Fig. 2.11), the atmospheric fluxes show strong annual cycles but the rates are one order of magnitude less than the inflow and outflow. Precipitation is about 40 mm/month in winter and reaches the maximum of 88 mm/month in September. In winter it accumulates on top of the ice to be released at the time of ice melting. The level of evaporation/sublimation is about 5 mm/month in winter and more than 100 mm/month in August–September. Transfer of water to the atmosphere is lowered also because

sublimation needs more power than evaporation and because the surface temperature becomes closer to the air temperature when ice grows thicker that lowers the turbulent fluxes. The averages are 56.9 mm/month and 43.3 m/month for precipitation and evaporation/sublimation, respectively.

Evaporation and sublimation are strongly limited by the available heat fluxes. In practice, in cold climate conditions the mass loss per unit area is less than 10 mm liquid water equivalent per day, while the average level is 1 mm/day. Evaporation takes place in open water and melt ponds, while dry snow and ice surfaces lose mass by sublimation. Occasionally atmospheric water vapour deposits as hoar crystals or condenses into liquid water on the surface that also brings the phase change energy to the surface. Latent heat transfer  $Q_e$  for evaporation or sublimation, respectively, can be directly expressed as

$$\begin{aligned} Q_e &= -\rho_i L_s E \text{ (ice)} \\ Q_e &= -\rho_w L_e E \text{ (water)} \end{aligned} \quad (2.17)$$

where  $\rho_w$  is water density. The latent heat of vaporization of liquid water depends on the temperature,  $L_e [\text{kJ kg}^{-1}] = 2,494 - 2.2 \cdot T [^\circ\text{C}]$ , the latent heat of freezing is  $L_f = 333.5 \text{ kJ kg}^{-1}$ , and the latent heat of sublimation is  $L_s [\text{kJ kg}^{-1}] = 2,828 - 0.39 \cdot T [^\circ\text{C}]$  ( $T \leq 0^\circ\text{C}$ ). Thus sublimation needs about 13.5 % more power than evaporation.

**Example 2.9.** For  $Q_e \sim -30 \text{ W m}^{-2}$ , we have  $E \sim 1 \text{ mm day}^{-1}$ . This energy flux can be estimated using turbulent transfer models. A common way is the bulk formula (Eq. 2.13c). For the relative humidity of air at 50 % and  $U_a \sim 10 \text{ ms}^{-1}$ , the latent heat loss is  $Q_e \sim 100 \text{ W m}^{-2}$  ( $E = 3 \text{ mm day}^{-1}$ ) at the temperature of  $0^\circ\text{C}$ , but at  $-20^\circ\text{C}$  the energy would be reduced to  $20 \text{ W m}^{-2}$  ( $E = 0.6 \text{ mm day}^{-1}$ ).

### 2.3.4 Budgets of Impurities

Closely connected to the water budget are the budgets of impurities, which are received by atmospheric deposition and inflow from the drainage basin and lost of by outflow. Evaporation and sublimation remove only pure water. In addition to the water fluxes, concentrations of impurities are changed by sedimentation/resuspension and biochemical processes.

Consider the mass of a given chemical substance in a lake,  $C = c \cdot S$ , where  $c$  is the mean concentration as mass/volume. The balance is therefore

$$\frac{d}{dt}(cS) = c_i I - c_o O + A P c_P + \int \phi dS \quad (2.18)$$

where  $c_i$ ,  $c_o$ ,  $c_P$  are the concentrations in inflow, outflow and precipitation, respectively, and  $\phi$  is the influence of biochemical processes, resuspension and sedimentation. The renewal

time for each substance can be defined in a manner similar to the flushing time of the water mass. Freezing has no influence on the total budgets of impurities, but the concentrations of the impurities are different in ice and water. Therefore, freezing and melting influence on the concentration of impurities in the surface water layer beneath the ice.

---

## **2.4 Ice-Covered Lakes**

### **2.4.1 Zonation of Freezing Lakes**

In regards with ice, lakes can be divided into three main zones: ice-free zone, seasonal lake ice zone, and perennial lake ice zone. Years in these zones are qualitatively different. Between the perennial and seasonal zone there is a quasi-perennial zone, where lakes sometimes have ice-free summer, and between seasonal and ice-free zones there is an ephemeral zone, where ice occurs but some years are ice-free. The boundary between the seasonally and perennially ice-covered lakes is quite thin, since there are not many lakes, which are seasonal but occasionally possess multi-year ice. Proglacial lakes can be taken as a sub-category in the perennial lake ice zone, as there the water body is always in contact with land ice.

### **2.4.2 Seasonal Lake Ice Zone**

The zone of seasonally freezing lakes covers large areas of the continents (Fig. 2.13). This zone is close to the diagram of Hutchinson and Löffler (1956), showing that lakes located between 40° and 80° latitudes may freeze in the seasonal cycle. Bates and Bilello (1966) estimated the southern boundary of seasonal ice cover in the Northern Hemisphere to follow approximately the latitude 45°N, higher in the Western Europe and lower in Asia and North America. In this latitude band there are also permanently ice-covered lakes in very high altitudes. Basically, where the mean air temperature in the coldest month is below the freezing point, shallow freshwater lakes are potential to freeze over (Fig. 2.2).

The seasonal ice zone can be further sub-classified into lakes with a stable ice or unstable ice cover. Lakes of the former class freeze over annually (Fig. 2.14), while in the latter class the ice cover breaks and full ice coverage is not necessarily achieved every year. This feature is lake-specific, since ice formation is strongly dependent on the regional climate conditions, as well as on the depth, size and morphology of the lake basin. For example, in the present climate in Europe, the whole Finland belongs to the stable ice zone, but two large lakes nearby, Ladoga (Prokacheva and Borodulin 1985) and Peipsi (Reinart and Pärn 2006), have unstable ice cover.

Apart from the ephemeral zone the mean annual maximum ice thickness in seasonally freezing lakes ranges within 20–200 cm. No reliable data exist on the maximum possible thickness of seasonal lake ice; based on the sea ice data from the Siberian shelf, it can be



**Fig. 2.13** The zone of seasonally freezing lakes in the northern hemisphere (Bates and Bilello 1966) and the 0 °C climatological isotherm taken from Fig. 2.1. The contours 100 and 180 refer to the mean length of the ice season (days)

estimated that the seasonal ice in Siberian lakes can grow to approximately 2 m during one winter (Kirillin et al. 2012). As a theoretical upper limit, Kirillin et al. (2012) refer to 270 cm based on the freezing-degree-days in the coldest place in the northern hemisphere (Oymakon, East Siberia). In medium-size lakes (10 km scale), the thickness of ice needs to be more than 10 cm to span a solid, stable ice sheet across the lake.

The ephemeral zone can be several latitude degrees wide. In eastern Europe such lakes are found south from about 55°N, e.g., in Northern Germany and Hungary. In this zone the nature as well as the people need to adapt life for both ice and ice-free winters. Winter 1963 was the latest very cold winter in Central Europe, and at this extreme, even the deep Lake Constance (Bodensee) bordering Austria, Germany and Switzerland froze over (Fig. 2.15).





**Fig. 2.14** Wuliangsuhai Lake in Inner Mongolia. In spite of the low latitude ( $40.5^\circ$ ), the lake freezes over annually and the ice thickness is about 1 m. *Photograph* Ms. Yang Fang, printed with permission



**Fig. 2.15** Lake Constance (Bodensee) froze over in winter 1963, and the ice was thick enough for cars and for pressure ridges to form (Zintz et al. 2009). *Photograph* by Mr. Julius Pietruske, printed by permission

### 2.4.3 Lakes with Perennial Ice

There are two categories of lakes with perennial ice. In very cold climate it is possible that at least some of the ice grown in winter survives over summer and becomes multi-year ice. The second category, proglacial lakes, contains liquid water bodies at side, on top and beneath glaciers or ice sheets and therefore these lakes are always in contact with land ice.

If not all ice melts in summer, the ice cover consists of first-year ice and multi-year ice. Example in Nunavut there are such lakes (Veillette et al. 2010). Occurrence of multi-year lake ice was observed in Colour Lake, Axel Heiberg Island, Nunavut (Adams et al. 1989) but it is there a rare event. Another lake sometimes possessing multi-year ice is Teshekpuk Lake in Alaska (Arp and Jones 2011). But to the author's knowledge, in the present climate, the coldest place in the Northern Hemisphere—Siberia—contains only seasonally ice-covered lakes. In summer, lake ice melts mainly due to the radiation balance, which may account for up to  $2\text{--}3\text{ cm day}^{-1}$  in ice thickness. Therefore, if the melting period is more than 100 days long, the melt volume will overcome the winter's ice growth. For a partial summer ice cover to survive, the conditions must be quite specific, since lakes have rather small dimensions. It may take place if a lake has bays sheltered from direct solar radiation etc. The partial ice cover state is something delicate between fully ice-covered state and seasonal ice cover (Fig. 2.16).

Perennially fully ice-covered lakes are found in very cold climate conditions, when the ice cover is snow-free and consists of clear ice, e.g., in the McMurdo Dry Valleys in Antarctica (Priscu 1998). Then the surface heat balance can be predominantly negative. Solar radiation heats the water body underneath, but the ice cover survives over summer. Due to the low thermal conductivity of ice, the absorbed heat does not escape easily, and accumulation of heat results in internal warming. This is similar to the so-called cool skin phenomenon in lakes and seas during calm and clear summer days. In the case of ice cover, the situation can be persistent, that leads to perennially ice-covered lakes. The ice cover in these lakes has been observed to be several meters thick, in Lake Vida the ice cover has been estimated as 20 m thick (Bar-Cohen et al. 2004).

There are three types of proglacial lakes connected to glaciers and ice sheets (e.g., Menzies 1995). *Epiglacial lakes* are found on the bare ground close to the boundary of the land ice mass (Kaup 1994); *subglacial lakes* are very old water bodies at the base of ice sheet (e.g., Siegert et al. 2001); and *supraglacial lakes* form in blue ice regions in the surface layer in summer (Winther et al. 1996; Bajracharya and Mool 2009; Leppäranta et al. 2013). Epiglacial lakes are as normal cold region lakes with a soil or rock bottom, fed mainly by glacial melt water inflow. They are an important habitat of life in the polar world. Normally these lakes have seasonal ice cover but blocks of glacial ice may be present.

Subglacial lakes are one of the most exciting geographical findings of the 20th century. The first evidence of their existence was from Soviet radio-echo soundings in the 1960s (see Priscu and Foreman 2009). Subglacial lakes are not yet well known but they form very specific physical and microbiological systems at the bottom of the Antarctic ice sheet. The water temperature is at the melting point corresponding to the ambient pressure,



**Fig. 2.16** In Schirmacher oasis, Dronning Maud Land, Antarctica there are lakes where lake ice may survive over summer. The picture shows such lake at the Russian Novolazarevskaya Station (70°49.3'S 11°38.7'E) in late summer, February 4, 2005

at about  $-2.5^{\circ}\text{C}$ . The water body must be in balance between the geothermal heat flux from the ground and conduction of heat through the overlaying ice sheet. The largest subglacial lake is Lake Vostok, located close to the Russian Vostok station.

Supraglacial lakes form and grow from the penetration of solar radiation into the ice sheet. For sufficient penetration, the surface needs to be ice and therefore these lakes form in glacial *blue ice* regions. The depth of seasonal supraglacial lakes is of the order of 1 m. When the surface heat balance is negative, the lake has an ice cover. They are extremely low in biota (Keskitalo et al. 2013). Supraglacial lakes are found on the Antarctic and Greenland ice sheets and in many mountain glaciers. In Greenland they are much more developed and have a major impact on the ice mass balance (Hoffman et al. 2011; Liang et al. 2012). If a supraglacial lake can preserve some of its water in liquid state over the winter, it starts a year-by-year growing stage. This would accelerate local melting, lead to lake growth and eventually catastrophic formation of fractures taking the water in and ending in a major change in the local glacial environment.

## 2.5 Lake Ice Climatology

As written in Sect. 2.2.4, freezing lakes can be divided into the following three main zones: perennial zone, seasonal zone, and ephemeral zone (Table 2.8). Considering the climatology of these zones, two binary variables are introduced (see Jevrejeva 2004): *Ice occurrence*  $I$ ,  $I(n) = 1$  (0) if ice occurs (does not occur) in ice year  $n$ , and *Open lake occurrence*  $O$ ,  $O(n) = -1$  (0) if ice year  $n$  is ice-free (is not ice-free). In fully seasonal lakes,  $I + O = 0$ , while in ice-free and perennially ice-covered lakes  $I + O$  equals  $-1$  and  $1$ , respectively. Note that in Sect. 2.1.1, the ice year was defined as the period between two consequent summer maxima of the lake heat content. There are long records of lakes freezing over in extreme years in relatively warm climate regions. Example Maurer (1924) reported of cases from southern Germany and Switzerland back to year 1400. In contrast, ice-free winters would provide information of extremely warm winters in the stable seasonal lake ice zone, but such records are not known to the author.<sup>9</sup>

Lake ice phenology studies the dates of freezing and ice breakup (Futter 2003). Their annual timing has been recorded for long periods in a large number of lakes due to practical reasons and due to general interest in nature phenomena (Magnusson et al. 2000). They are most eye-striking events with major impacts on the nature and society. Also lake ice phenology is a good climatic indicator due to its sensitivity to the climate conditions and the existence of long records (e.g., Robertson et al. 1992; Livingstone 2000; Duguay et al. 2006; Korhonen 2006; Karetnikov and Naumenko 2008; Bernhardt et al. 2011). To be precise, some basic definitions of ice phenology are first needed.

The *freezing date* is defined as the first day in an ice season when the observation area has frozen over. Often this date refers to the freeze-over of the whole lake, but in larger lakes observations do not necessarily cover the whole water body. The *freeze-up date*, also called ice-on date, is used for the first day of complete coverage of ice in a given season. The *ice break-up date*, also called ice-off date, in turn, is the last ice day in a given winter season. The *length of ice season* is the time between the freezing and breakup dates, while the *number of ice days* is the number of days when ice actually exists. Care should be taken in conducting a comparative analysis whether the freezing date or freeze-up date has been consistently used. Their difference can be appreciably long, especially in large and deep lakes.

An example of a phenomenological time series is given in Fig. 2.17 showing typical features in boreal lakes. In Lake Kallavesi (left) the variability of the freezing date is  $2\frac{1}{2}$  months, and for the breakup date it is 1 month. For the last 100 years most lake ice time series show slow trends toward milder winters with high random variability. Toward the climatological ice margin in Lake Stechlin (right) the variability of the freezing and breakup date increases and ice-free winters become more common.

Ice formation is generally governed by intense radiative and turbulent heat losses from the warmer lake surface to the colder atmosphere. The stratification in the atmospheric surface layer is unstable and turbulent losses can be large. When the water temperature is

<sup>9</sup> In Finland, all lakes have frozen over every year, except possibly some deep basins in 1930.

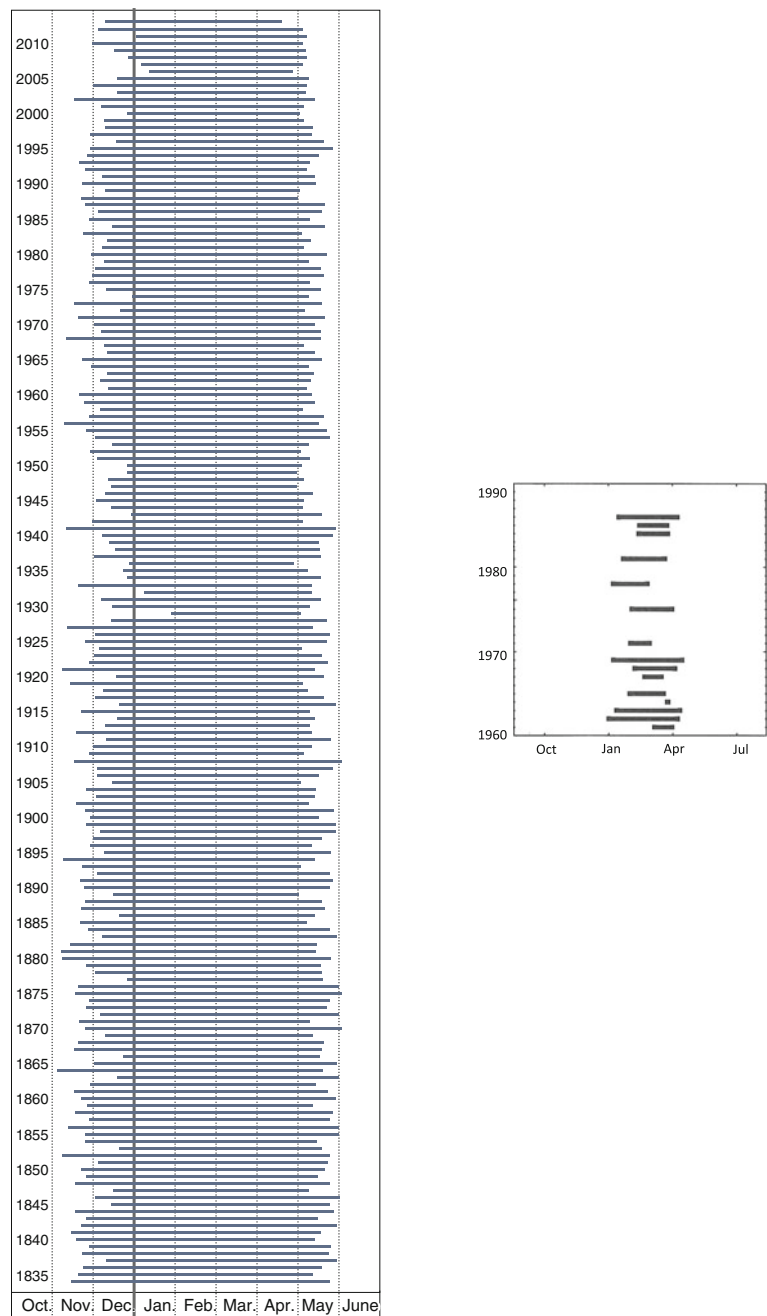


**Fig. 2.17** Lake ice phenology time series for Lake Kallavesi, Finland (63°N 28°E), 1835–2013 and Lake Stechlin, Germany (53°N 13°E), 1960–1990; Lake Kallavesi data are from SYKE (Finnish Environment Institute) data base and Lake Stechlin data are from Kirillin et al. (2012) based on Bernhardt et al. (2011). The *thick lines* show the annual ice season from freezing to ice breakup

above the temperature of the maximum density ( $T_m$ ), the lake water column is unstable in cooling, thermocline deepens and heat is removed from the deep water. Due to mechanically forced mixing, convection can continue at  $T < T_m$ . Finally, inverse stratification develops with surface layer close to the freezing point and a little warmer lower layer. Heat transport from the warm deeper layers to the lake surface is reduced, the surface cooling rate increases, and the surface temperature achieves the freezing point, followed by ice formation. Hence, the timing of freezing is strongly dependent on synoptic conditions—passages of cold air masses and strong winds—over the lake. In deep lakes, the convective phase can last long, even through the whole winter.

The heat balance during ice melting is fundamentally different from that during lake cooling and ice growth (Jakkila et al. 2009). Then the stable stratification of atmospheric surface layer strongly reduces the turbulent heat exchange at the lake–air interface. Solar radiation is the dominant source of heat for snow and ice melting, partly absorbed by the ice sheet and partly by the lake water below. This fact implies also that albedo and transparency of the ice sheet have a strong influence on melting. The key role of the solar radiation also explains the fact that ice breakup date is coherent at spatial scales of hundreds of kilometres (Magnuson et al. 2000). Other factors able to efficiently accelerate ice melting are liquid precipitation and strong and warm winds.

The sequence of an ice season, from the first freezing to the final break-up is not a simple cycle but there may be melt–refreeze events in between (Bernhardt et al. 2011; Kirillin et al. 2012). Ice formation and melting are not symmetric processes but ice is self-protecting. Once an ice cap has formed, it is difficult to melt it in since in winter solar radiation level is low and albedo feedback keeps the absorption of solar radiation low. Also the lake heat storage is largely isolated from the ice by weak mixing conditions. But still it is possible that ice cover disappears and forms again within one ice season, even several times. This is especially true in the vicinity of the climatological margin of freezing lakes. Then the freezing date and breakup date are still defined as the first and last ones in the ice season, and the presence of ice-free periods is seen in the difference between the length of ice season and the number of ice days. In the other extreme, in a cold year at high-latitudes or high-altitudes, it is possible that some ice survives over summer and becomes multi-year ice. The ice cover has then changed into perennial state.

Because of the heat budget, freeze-up of lakes depends on the lake depth and size, while melting is more up to the growth of ice and snow accumulation during winter. Therefore, ice breakup date follows closely the latitude, but individual lake characteristics show up in the freezing date (Fig. 2.18).

After ice cover formation, ice thickness increases as long as the released latent heat from freezing and the heat flux from the water body can be conducted through the ice to the atmosphere (e.g., Leppäranta 2009a). The main factors controlling the ice growth are the heat fluxes at the upper and lower boundaries of the ice cover together with the thermal properties of ice and snow. An early appearance of snow cover can play a crucial role in decelerating the ice growth due to the very low heat conductivity of snow. The total thickness of ice as well as the thicknesses of congelation ice and snow-ice layers is



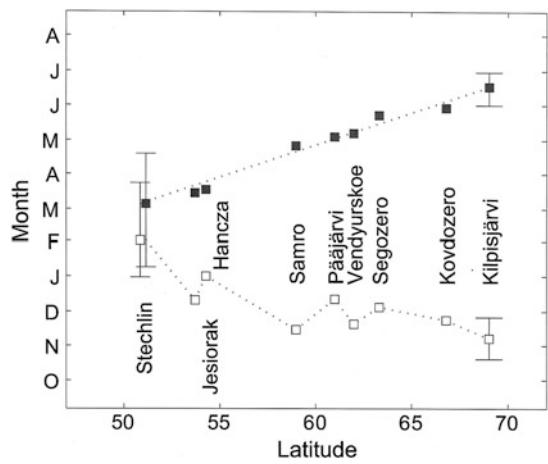


**Fig. 2.18** Long-term averages of ice-on (*white squares*) and ice-off (*black squares*) in several European lakes (Kirillin et al. 2012). Data are from: Lake Stechlin, Germany, 1961–2002 (Bernhardt et al. 2011); Lakes Jesiorak and Hancza, Poland, 1961–2000 (Marszelewski and Skowron 2006); Lakes Samro, Segozero, and Kovdozero, Russia, 1936–1989 (Efremova and Palshin 2011); Lake Vendyurskoe, Russian Karelia, 1994–2000 and 2007–2011 (Terzhevik, unpublished); Lake Pääjärvi, Finland, 1910–1988 (Kärkäs 2000); and Lake Kilpisjärvi, Finland, 1964–2008 (Lei et al. 2012). The *error bars* for Lakes Stechlin and Kilpisjärvi show the earliest and the latest observed values

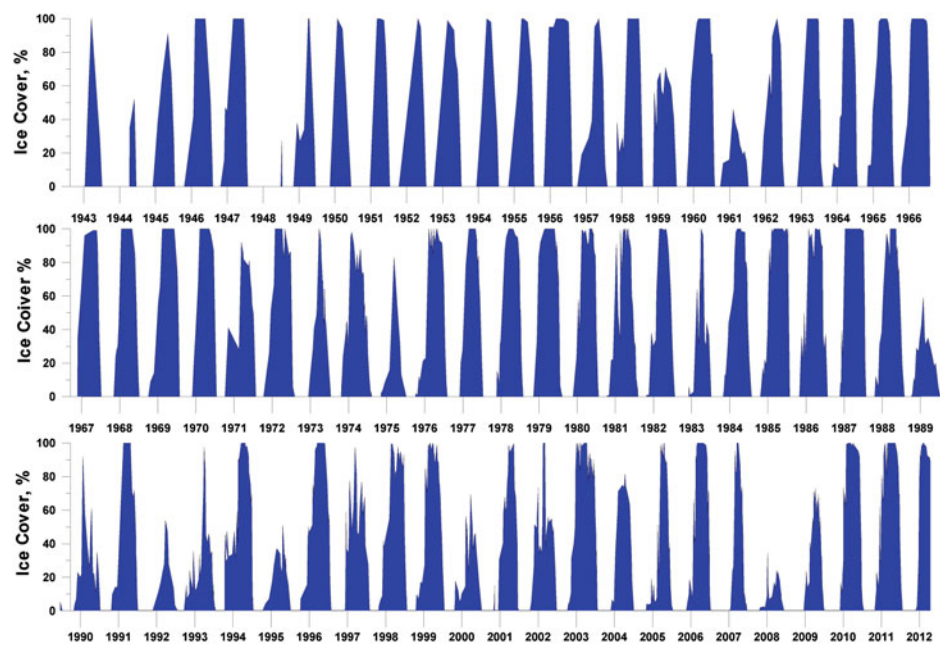


**Fig. 2.19** Year-to-year variation of ice cover of Lake Ladoga from 1943 to 2010 (1944 and 1948 are missing) using various sensors from airplane and satellites (Karetnikov and Naumenko 2011; Karetnikov et al. 2015)



primarily controlled by the air temperature and snowfall time history. The general trend towards warmer winters in ice phenology may thus not be easy to detect in the ice thickness data (e.g., Leppäranta and Seinä 1985; Jevrejeva et al. 2004). Evolution of ice coverage is related to ice thickness in that thicker ice has more lateral strength and a thick enough ice cover does not break any more before the melting phase.

The severity of winters can be quantified with the *maximum annual ice thickness*. In large lakes, the period of lateral ice growth may be long, and therefore the quantity *ice coverage*, equal to the ice area divided by the total lake area, is another characteristic of the severity of the ice season. Example in Lake Ladoga the probability of complete ice coverage is about 50 %, although ice forms in the lake every year (Prokacheva and Borodulin 1985; Karetnikov and Naumenko 2008, 2011) (Fig. 2.19).

Freezing of Lakes and the Evolution of their Ice Cover

Leppäranta, M.

2015, X, 301 p. 136 illus., 90 illus. in color., Hardcover

ISBN: 978-3-642-29080-0